Reversible Ca Gradients between the Subplasmalemma and Cytosol Differentially Activate Ca-dependent Cl Currents

Khaled Machaca and H. Criss Hartzell

From the Department of Cell Biology, Emory University School of Medicine, Atlanta, Georgia 30322-3030

ABSTRACT *Xenopus* oocytes express several different Ca-activated Cl currents that have different waveforms and biophysical properties. We compared the stimulation of Ca-activated Cl currents measured by two-microelectrode voltage clamp with the Ca transients measured in the same cell by confocal microscopy and Ca-sensitive fluorophores. The purpose was to determine how the amplitude and/or spatio-temporal features of the Ca signal might explain how these different Cl currents were activated by Ca. Because Ca release from stores was voltage independent, whereas Ca influx depended upon the electrochemical driving force, we were able to separately assess the contribution of Ca from these two sources. We were surprised to find that Ca signals measured with a cytosolic Ca-sensitive dye, dextran-conjugated Ca-green-1, correlated poorly with Cl currents. This suggested that Cl channels located at the plasma membrane and the Ca-sensitive dye located in the bulk cytosol were sensing different [Ca]. This was true despite Ca measurement in a confocal slice very close to the plasma membrane. In contrast, a membrane-targeted Ca-sensitive dye (Ca-green-C_{18}) reported a Ca signal that correlated much more closely with the Cl currents. We hypothesize that very local, transient, reversible Ca gradients develop between the subplasmalemmal space and the bulk cytosol. [Ca] is higher near the plasma membrane when Ca is provided by Ca influx, whereas the gradient is reversed when Ca is released from stores, because Ca efflux across the plasma membrane is faster than diffusion of Ca from the bulk cytosol to the subplasmalemmal space. Because dissipation of the gradients is accelerated by inhibition of Ca sequestration into the endoplasmic reticulum with thapsigargin, we conclude that [Ca] in the bulk cytosol declines slowly partly due to futile recycling of Ca through the endoplasmic reticulum.

KEY WORDS: store-operated Ca entry • voltage clamp • calcium imaging • *Xenopus* • oocyte

INTRODUCTION

Many G protein– and tyrosine kinase–associated receptors stimulate phospholipase C and the production of inositol 1,4,5-trisphosphate (IP_3),[1] resulting in a rise in cytosolic Ca ($[Ca]_c$). The rise in $[Ca]_c$ in response to activation of these receptors is typically biphasic, starting with a transient increase due to IP_3-stimulated Ca release from internal endoplasmic reticulum (ER) stores, followed by a long lasting $[Ca]_c$ rise due to entry of extracellular Ca through store-operated Ca channels (Putney, 1990; Pozzan et al., 1994; Parekh and Penner, 1997). Ca entry through this pathway is termed store-operated Ca entry (SOCE), formerly known as capacitative Ca entry (Putney, 1986). Ca often participates in multiple signaling pathways that are each controlled by different extracellular signals in the same cell. For example, Ca controls phototaxis, mating, and deflagellation in the single-celled alga *Chlamydomonas* (Quarmby and Hartzell, 1994), mechanosensitivity and afferent and efferent synaptic transmission in vertebrate hair cells (Lenzi and Roberts, 1994), and gene expression and synaptic transmission in neurons (Ghosh and Greenberg, 1995; Finkbeiner and Greenberg, 1996; Bito et al., 1997). A fundamental problem in Ca signal transduction involves understanding how these different pathways are kept separate and how different effector systems discriminate between Ca signals. There is growing evidence that spatial, temporal, and amplitude factors are involved in the process of Ca signal discrimination. For example, certain Ca signals may be specifically localized to microdomains that contain the appropriate effector molecules (Thorn, 1996; Rios and Stern, 1997; Landolfi et al., 1998; Neher, 1998). Spatial separation of Ca signals is often achieved by localization of the Ca sources and sinks, which include Ca buffers that restrict the diffusion of Ca. Specificity of Ca signals is also encoded in how effectors respond most efficiently to Ca. Certain effectors respond optimally to frequency-modulated Ca oscillations, whereas others respond to steady state Ca elevations (Hajnoczky et al., 1995; Thomas et al., 1996; Berridge, 1997b; Bito et al., 1997; Dolmetsch et al., 1997; Deisseroth et al., 1998; De Koninck and Schulman, 1998).

Xenopus oocytes express several endogenous Ca-activated Cl currents that have different waveforms and

Address correspondence to H. Criss Hartzell, Department of Cell Biology, Emory University School of Medicine, Atlanta, GA 30322-3030. Fax: 404-727-6256; E-mail: criss@cellbio.emory.edu

[1]*Abbreviations used in this paper:* ER, endoplasmic reticulum; IP_3, inositol 1,4,5-trisphosphate; SERCA, sarcoplasmic-ER Ca ATPase; SOC, store-operated Ca channel; SOCE, store-operated Ca entry.

J. Gen. Physiol. © The Rockefeller University Press • 0022-1295/99/02/249/18 $2.00
Volume 113 February 1999 249–266
http://www.jgp.org

biophysical properties (Miledi and Parker, 1984; Parker et al., 1985; Gillo et al., 1987; Dascal, 1987; Parker and Miledi, 1987a,b; Snyder et al., 1988; Berridge, 1988; Boton et al., 1989; Parker and Ivorra, 1991; Hartzell, 1996). We have characterized three Ca-activated Cl currents: a noninactivating outward Cl current ($I_{Cl1\text{-}S}$) that is activated by Ca released from stores, and a slow inward Cl current (I_{Cl2}) and a transient outward Cl current ($I_{Cl1\text{-}T}$) that are activated by Ca influx through store-operated Ca channels (Hartzell, 1996). The presence of multiple currents with distinct properties could be explained by the presence of several types of channels or by a single channel whose properties depend upon the concentration and/or spatio-temporal features of the Ca signal that activates it (Kuruma and Hartzell, 1998).

The Cl currents in *Xenopus* oocytes offer an excellent opportunity to understand how different Ca signals ultimately result in physiologically different responses. Our objective here was to determine how Ca-activated Cl currents were related to changes in cytosolic Ca stimulated by IP_3 injection into the oocyte. We were surprised to find that the correlation between Ca signals measured using a cytosolic Ca-sensitive dye, dextran-conjugated Ca-green-1, and Cl currents was quite poor. Analysis of these results suggested that Cl channels, which were located at the plasma membrane, were sensing different Ca than was detected by the Ca-sensitive dye, which was located in the bulk cytosol. This was true even though we were measuring Ca using confocal microscopy in a slice of oocyte very close to the plasma membrane. We demonstrated the presence of transient Ca gradients between bulk cytosol and plasmalemma by showing that a membrane-targeted Ca-sensitive dye (Ca-green-C_{18}) reported a Ca signal that correlated much more closely with the Cl currents. We hypothesize that these transient gradients arise because Ca efflux across the plasma membrane is faster than diffusion of Ca from the bulk cytosol to the subplasmalemmal space. This slow diffusion is partly due to the gigantic size of the oocyte (~1 mm diameter). In addition, we find that slow Ca clearance from the cytoplasm plays a role in maintaining these transient gradients. This slow decline of cytosolic Ca levels is due to futile recycling of Ca through the endoplasmic reticulum.

MATERIALS AND METHODS

Isolation of Xenopus Oocytes

Stage V–VI oocytes were harvested from adult albino (or normal) *Xenopus laevis* females (Xenopus I) as described by Dascal (1987). *Xenopus* were anesthetized by immersion in Tricaine (1.5 g/liter). Ovarian follicles were removed and digested in normal Ringer with no added calcium, containing 2 mg/ml collagenase type IA (Sigma Chemical Co.), for 2 h at room temperature. The oocytes were extensively rinsed with normal Ringer, placed in L-15 medium (GIBCO BRL), and stored at 18°C. Oocytes were usually used between 1 and 5 d after isolation.

Imaging and Electrophysiological Methods

Methods are described in detail in Hartzell (1996) and Machaca and Hartzell (1998). In brief, *Xenopus* oocytes were injected with 23 nl Ca-green-1 coupled to 70 kD dextran (333 μM) for a final calculated oocyte concentration of ~7.6 μM, or with 13 nl Ca-green-C_{18} (333 μM) and voltage-clamped with two microelectrodes as described in Fig. 1. Confocal images were acquired using a Zeiss LSM 410 confocal box fitted to a Zeiss Axiovert 100TV inverted microscope using a Zeiss 10× objective (0.5 NA). For Ca-green-dextran, the pinhole was fully open, resulting in a focal section of 1,275 × 1,275 × 35 μm illustrated by the hatched box in Fig. 1 a. For Ca-green-C_{18}, the focal section was 200 × 1,275 × 4 μm. Image data was analyzed using NIH image 1.60 on a Mac IIfx and voltage-clamp data was analyzed on a Pentium PC using Origin 5.0 (Microcal Software). For plots of Ca fluorescence, the fluorescence intensity of the entire confocal section was averaged and expressed as a ratio of the background fluorescence taken either before IP_3 injection or extracellular Ca addition, depending on the experimental design. Experiments were performed at room temperature (22–26°C). The extracellular solutions used were (mM): normal Ringer, 123 NaCl, 2.5 KCl, 1.8 $CaCl_2$, 1.8 $MgCl_2$, 10 HEPES, pH 7.4; and Ca-free Ringer solution, which was the same except that $CaCl_2$ was omitted, $MgCl_2$ was increased to 5 mM, and 0.1 mM EGTA was added.

Endogenous Ca activated Cl currents, referred to as $I_{Cl1\text{-}S}$, I_{Cl2}, and $I_{Cl1\text{-}T}$ were measured as described in Fig. 1 b. $I_{Cl1\text{-}S}$ (current at the end of the first +40-mV pulse, Fig. 1 b) is a sustained outward current at depolarizing potentials that is activated quickly (~10 s) after IP_3 injection by Ca released from intracellular stores and has an outwardly rectifying steady state current–voltage relationship. I_{Cl2} (maximum current during the −140-mV pulse, Fig. 1 b) is an inward current that is activated by Ca entry through store-operated Ca channels (SOCs) driven by the negative membrane potential and has an inwardly rectifying steady state current–voltage relationship. $I_{Cl1\text{-}T}$ is a transient outward current (peak outward current during the second +40 mV pulse, Fig. 1 b) that was activated by a depolarizing pulse preceded by a hyperpolarizing pulse to stimulate Ca influx. For a more detailed characterization of the Cl currents, see Hartzell (1996), Machaca and Hartzell (1998), and Kuruma and Hartzell (1999).

RESULTS

Voltage Dependence of Ca Entry

The first goal was to characterize the Ca signal which was caused by Ca influx through SOCs. Ca influx through SOCs was measured by imaging Ca in oocytes injected with dextran-conjugated Ca-green-1 using confocal scanning microscopy while voltage clamping the oocyte with a two-microelectrode voltage clamp. The confocal fluorescence image reported cytoplasmic Ca primarily because the injected 70-kD–coupled Ca-green-1 is too large to partition into organelles (Luby-Phelps, 1989; Girard and Clapham, 1993; Camacho and Lechleiter, 1993; Jouaville et al., 1995). We also used Ca-green-5N, which has a lower Ca affinity, and obtained identical results. The oocyte was voltage clamped at a holding potential of 0 mV and pulsed to potentials between −140 and +120 mV for 1 s

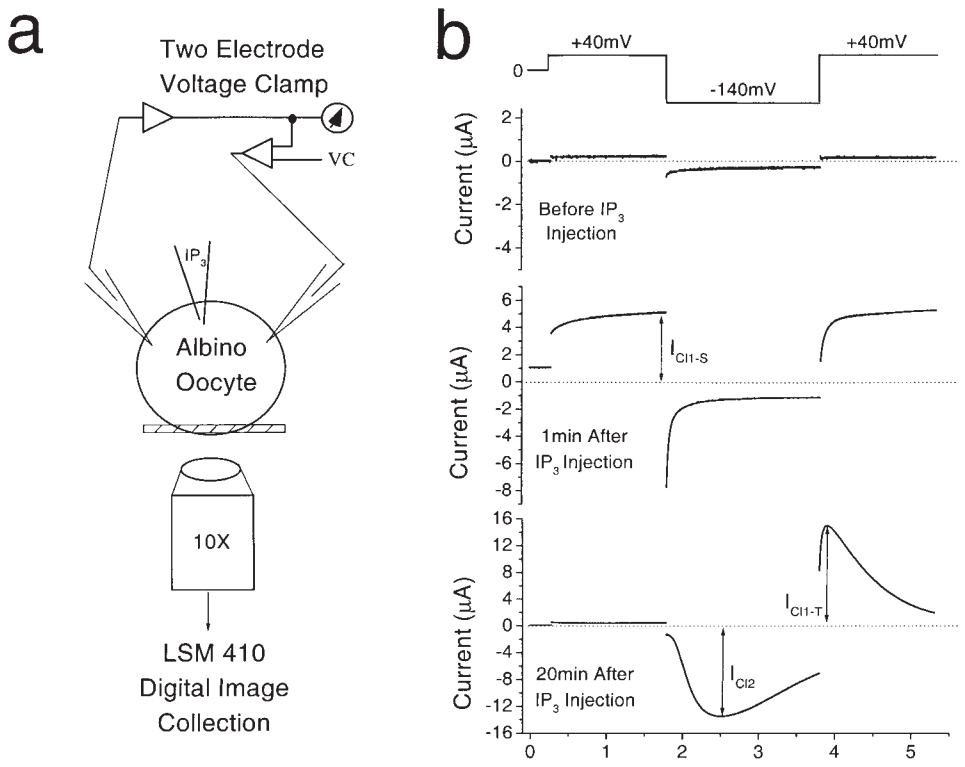

FIGURE 1. Experimental setup. (a) Albino *Xenopus* oocytes were voltage clamped by two electrodes and simultaneously imaged by confocal microscopy using an LSM 410 confocal box (Carl Zeiss, Inc.). A third electrode was used to inject IP_3 and release intracellular Ca stores. The hatched box represents the focal section of the oocyte imaged when the pinhole was open to the maximum. (b) Ca-dependent Cl currents. The voltage protocol used in most of the experiments is shown at top. The cell was held at 0 mV and stepped to +40 mV (referred to as +40 mV[1]), −140 and +40 mV again (+40 mV[2]). The currents elicited by this voltage protocol at different time points are shown. Before IP_3 injection, the baseline currents are shown. Injection of IP_3 releases Ca from internal stores and activates $I_{Cl1\text{-}S}$, an outward current that does not inactivate for the duration of the pulse. $I_{Cl1\text{-}S}$ is measured as the current at the end of the first +40 mV pulse as illustrated in the middle panel. Note that during the Ca release phase $I_{Cl1\text{-}S}$ is also observed during the second +40-mV pulse. After store depletion, SOCE is activated and Ca influx activates I_{Cl2}, an inward current upon hyperpolarization to −140 mV and $I_{Cl1\text{-}T}$, a transient outward current detected during the second +40-mV pulse. I_{Cl2} and $I_{Cl1\text{-}T}$ are measured as the maximum current during the −140-mV and second +40-mV pulse, respectively. $I_{Cl1\text{-}T}$ is observed only when the +40-mV pulse is preceded by the −140-mV step to induce Ca influx.

at 30-s intervals. Before IP_3 injection, the Ca fluorescence (F_{Ca}/F_0) was very small and was independent of voltage (not shown). However, if we allowed enough time after IP_3 injection for store depletion and activation of SOCE (~10 min), the Ca signal increased significantly with membrane hyperpolarization (Fig. 2 a, ○). We believe that the voltage-dependent Ca fluorescence reflected the accumulation of Ca in the oocyte due to Ca influx through SOCs because the Ca fluorescence was dependent on extracellular Ca (Fig. 2 a, ■) and the voltage dependence of the Ca fluorescence corresponded closely to the voltage dependence of the store-operated Ca current (I_{SOC}) we have previously characterized electrophysiologically (Hartzell, 1996; Yao and Tsien, 1997; Kuruma and Hartzell, 1999; Fig. 2 b). I_{SOC} resembled the prototypic SOC current, I_{CRAC}: it strongly inwardly rectified with a positive reversal potential (Hoth and Penner, 1993; Yao and Tsien, 1997).

The voltage-dependent Ca fluorescence was also stimulated by depleting intracellular Ca stores independently of IP_3. Treatment with ionomycin (Fig. 2 a, △), a Ca ionophore that selectively releases Ca from ER Ca stores (Morgan and Jacob, 1994), or prolonged treatment with thapsigargin, which blocks the ER Ca-ATPase and depletes Ca stores passively by unopposed leak of Ca out of the stores (Bird et al., 1992), stimulated voltage-dependent Ca fluorescence.

Ca Release from Stores Is Voltage Independent

If Ca release from stores is voltage independent, then the voltage dependence of the Ca signal caused by Ca influx provides a means to separate the fluorescence signals due to Ca influx and Ca release from stores. We therefore tested whether IP_3-induced Ca release from stores was voltage independent by comparing the Ca fluorescence at +40 and −140 mV when the oocyte was bathed in Ca-free solution so that there could be no Ca influx. Fig. 3 a shows pairs of images taken during the +40- and −140-mV pulses at different times during the experiment and a thresholded image (Δ) that shows the difference between the images at −140 and +40 mV. IP_3 injection (at 1 min) released Ca in a wave that swept through the entire oocyte (2.5 min) as described by Lechleiter and Clapham (1992). The Ca wave eventually subsided (10 min). The amplitudes of the Ca fluorescence at +40 and at −140 mV during the wave of Ca release were not significantly different (Fig. 3 b).

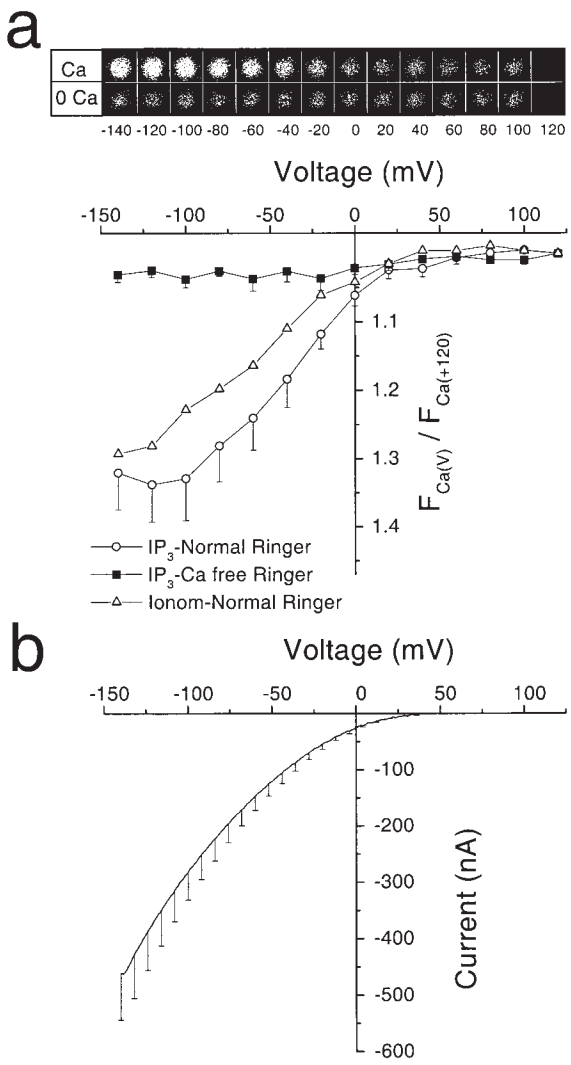

FIGURE 2. Visualization and voltage dependence of store-operated Ca entry. (a) Ca dynamics were imaged by confocal microscopy from a cell injected with Ca-green-1 coupled to 70 kD dextran and voltage clamped. Internal Ca stores were depleted of Ca by injection of 23 nl IP_3 (1 mM) (■ and ○) or by exposure to 14 μM ionomycin (△). 10 min after IP_3 injection, after the wave of Ca release and the development of store-operated Ca entry, the membrane potential was stepped to the indicated voltages from a holding potential of 0 mV (○). The same voltage protocol was repeated after switching the cell to Ca-free solution (■). The top shows the images of a representative experiment with the voltage indicated below the image. The Nernst equation predicts no influx at +120 mV. Therefore, the image at +120 mV was taken as background fluorescence and was subtracted from the images at the other voltages. In the bottom, total fluorescence at each voltage was measured and normalized to the fluorescence at +120 mV. Fluorescence intensity was plotted (mean ± SEM) as a function of voltage (n = 4) for Ca-free (■) and Ca-containing (○) solution. (b) Current–voltage relationship for I_{SOC} measured by a ramp voltage pulse from −150 to +100 mV from cells loaded with 5 mM BAPTA to inhibit the Ca-activated Cl currents, and voltage clamped. The mean current ± SEM was plotted as a function of voltage (n = 4).

This shows that Ca release from stores was independent of voltage. Voltage-dependent Ca fluorescence (Fig. 3 c) was shown to require Ca entry because addition of Ca to the bath (14.5 min) resulted in an abrupt increase in Ca fluorescence at −140 mV, whereas the fluorescence at +40 mV changed only slightly (Fig. 3 b). Operationally, store-operated Ca entry has been defined as the increase in Ca fluorescence observed upon addition of Ca to the bathing solution after internal stores have been depleted in Ca-free solution (Putney, 1990; Meldolesi et al., 1991). On the basis of this definition, the voltage-dependent Ca fluorescence we observe in Fig. 3 is store-operated Ca entry. However, clearly, Ca fluorescence does not measure Ca influx directly, but rather measures the accumulation of Ca, which is the final result of influx, efflux, equilibration with Ca buffers, Ca-induced Ca release from stores, and sequestration.

Ca-induced Ca Release Contributes Negligibly to the Voltage-dependent Ca Fluorescence

Ca influx can trigger Ca release from stores in *Xenopus* oocytes (Yao and Parker, 1993, 1994) as a result of the synergistic interaction of IP_3 and Ca on the IP_3 receptor (Iino, 1990; Parker and Ivorra, 1990; Bezprozvanny et al., 1991; Finch et al., 1991). Thus, the voltage-dependent Ca fluorescence could be a combination of Ca entry and subsequent release of additional Ca from stores not completely depleted by the IP_3 injection. Contribution of Ca-induced Ca release (CICR) to the voltage-dependent Ca signal was assessed in Fig. 3 by adding ionomycin to release any Ca remaining in stores after IP_3 injection. Ionomycin had no effect on fluorescence at either +40 or −140 mV or the voltage-dependent Ca signal (Fig. 3, a–c). Thus, CICR contributes negligibly to the voltage-dependent Ca fluorescence after IP_3 injection because IP_3 virtually depletes the stores.

Correlation between Ca Fluorescence and Cl Currents

Xenopus oocytes possess several Ca-activated Cl currents that have been used as real-time detectors of Ca at the plasma membrane (Miledi and Parker, 1984; Parker et al., 1985; Gillo et al., 1987; Dascal, 1987; Parker and Miledi, 1987a,b; Berridge, 1988; Snyder et al., 1988; Boton et al., 1989; Parker and Ivorra, 1991; Hartzell, 1996). The development of these currents and their relationship to cytosolic Ca after IP_3 injection are shown in Fig. 4. The oocyte was initially bathed in Ca-free solution and voltage clamped from a holding potential of 0 mV with a three-step episode consisting of steps to +40 mV for 1 s, −140 mV for 2 s, and +40 mV for 1 s with an interpulse interval of 26 s. The first +40 mV step is labeled +40 mV[1], and the second +40 mV[2]. See

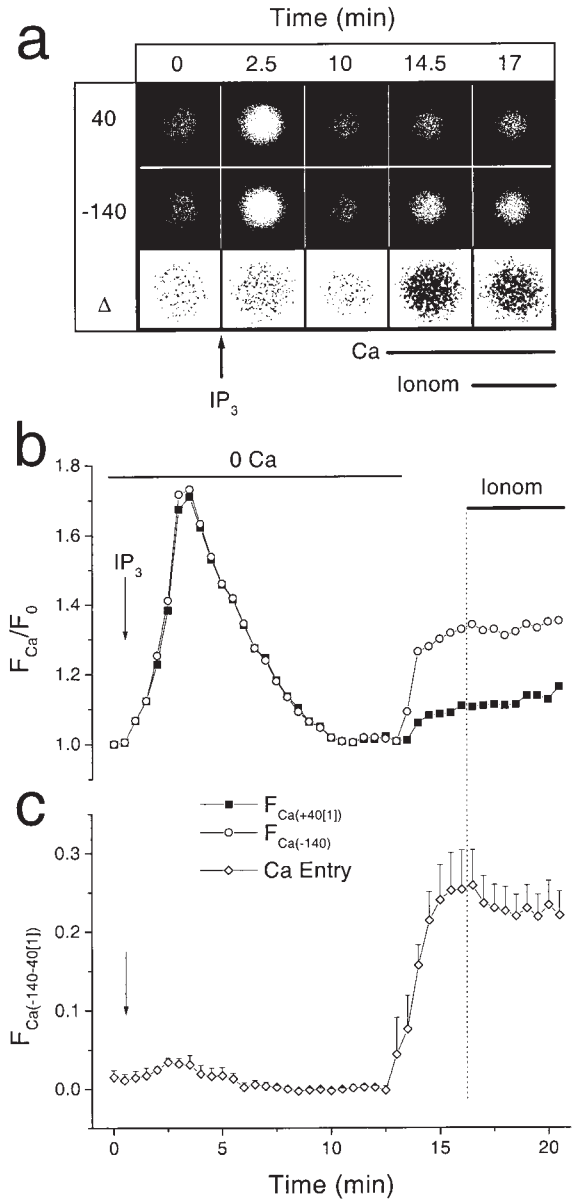

FIGURE 3. Voltage-independence of Ca release from stores. The oocyte was loaded with 7.6 μM Ca-Green-1–dextran, and stepped to +40 mV for 1 s, −140 mV for 2 s, and +40 mV again for 1 s from a holding potential of 0 mV at an interepisode interval of 26 s (30 s total per cycle). The cell was bathed in normal Ringer except where indicated by the bar showing Ca-free Ringer. (a) Confocal images collected 600 ms after the beginning of each pulse. Images collected at +40 mV, −140 mV and the difference (Δ) between the two images are shown. The difference (Δ) images are shown as binary images to better illustrate increased Ca levels. (b) IP_3 (23 nl, 1 mM) was injected at the arrow. Ca fluorescence during the +40-mV[1] (■) and −140-mV (○) pulse is plotted vs. time for a typical experiment. IP_3 injection stimulated an increase in Ca fluorescence that was independent of voltage. Approximately 8 min later, the cell was switched to Ca-containing Ringer, which produced a voltage-dependent change in the Ca fluorescence. The Ca ionophore, ionomycin (14 μM) was added to completely deplete intracellular Ca stores, as indicated. Ionomycin produced little effect. (c) Voltage-dependent Ca fluorescence as a function of time. Voltage-dependent Ca fluorescence was calculated as the difference between F_{Ca}/F_0 at −140 mV and +40 mV[1] (◇, average of four experiments).

MATERIALS AND METHODS and Fig. 1 for details of Cl currents measurement. Immediately after IP_3 injection, $I_{Cl1\text{-}S}$ was activated during both +40 mV steps of the episode (Fig. 4, a and b, trace a) and the Ca-green fluorescence (Fig. 4 c) increased in a voltage-independent manner at all potentials. The activation of $I_{Cl1\text{-}S}$ preceded the increase in Ca fluorescence (Fig. 4 d). This was at least partly due to the fact that Cl currents were measured from the entire cell, whereas the confocal image was obtained from a superficial optical slice at the pole opposite to the site of IP_3 injection (see Fig. 1). Therefore, the Ca fluorescence reached its maximum more slowly than $I_{Cl1\text{-}S}$ due to the time required for the Ca wave to travel from the injection site to the confocal plane (Machaca and Hartzell, 1998). More surprisingly, $t_{1/2}$ of decay of Ca fluorescence was approximately seven times slower ($P < 0.005$; $n = 7$) than the $t_{1/2}$ of decay of $I_{Cl1\text{-}S}$ (3.78 ± 0.68 vs. 0.52 ± 0.05 min) (Fig. 4 d, inset). Addition of Ca to the bath increased the voltage-dependent Ca fluorescence, which was stable for at least 15 min (Fig. 4 e). The amplitude of the voltage-dependent Ca fluorescence (Ca entry) was quite small compared with the voltage-independent Ca fluorescence (Ca release). In contrast, the $I_{Cl1\text{-}T}$ current activated by Ca entry was larger than the current activated by Ca release ($I_{Cl1\text{-}S}$).

Although the voltage-dependent Ca fluorescence correlated relatively well with both $I_{Cl1\text{-}T}$ and I_{Cl2} when Ca was added after the SOCE mechanism was fully activated (Fig. 4 f), the correlation between I_{Cl2} and Ca fluorescence was poor when one examined their temporal development after IP_3 injection (Fig. 5). Fig. 5 shows the results of an experiment in which the oocyte was bathed in normal Ca-containing solution from the onset of the experiment. Injection of IP_3 rapidly stimulated $I_{Cl1\text{-}S}$ (Fig. 5, a and b). As $I_{Cl1\text{-}S}$ returned to baseline, $I_{Cl1\text{-}T}$ and I_{Cl2} developed (Fig. 5, a and b). Concomitant with the injection of IP_3, there were large increases in Ca fluorescence during both +40- and −140-mV pulses (Fig. 5 c) that closely resembled the wave of Ca release seen in oocytes bathed in Ca-free solution (Fig. 4 c). The amplitudes of the Ca fluorescence during the +40- and −140-mV pulses were identical during the wave of Ca release, but shortly after the peak of the Ca release wave, the −140-mV Ca fluorescence became greater than the +40-mV[1] Ca fluorescence (Fig. 5 c) as SOCE developed (Fig. 5 d). Voltage-dependent Ca fluorescence was apparent immediately after Ca release from stores and increased gradually over a period of ~5 min to reach a plateau that remained stable for at least 20 min (Fig. 5 d). Both voltage-dependent Ca fluorescence and the Cl currents were abolished when the cell was switched to Ca-free solution (Fig. 5, a–d). The time course of development of $I_{Cl1\text{-}T}$ and voltage-dependent Ca fluorescence were very simi-

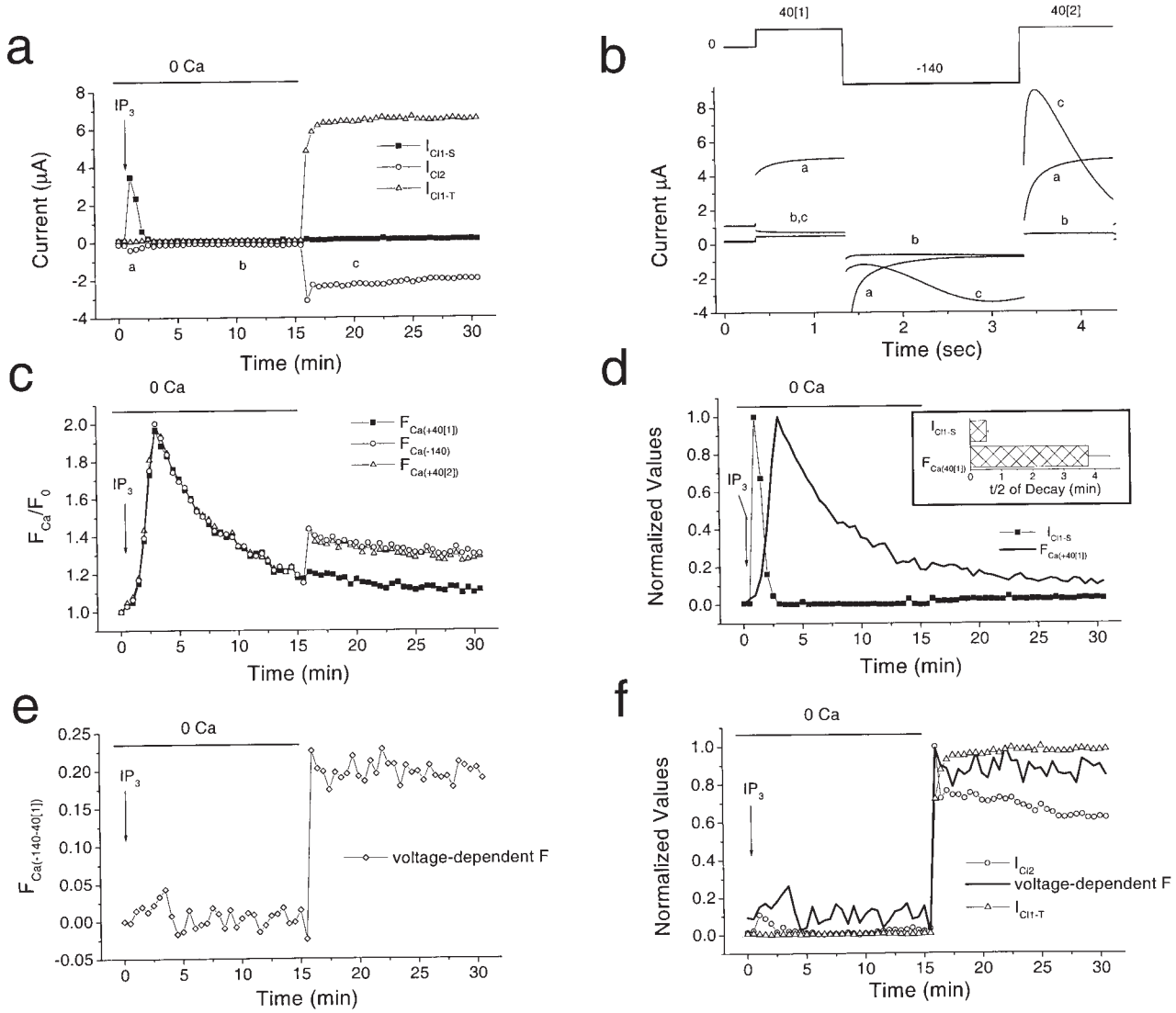

FIGURE 4. Correlation of Ca transients with Cl currents. The oocyte was loaded with 7.6 μM Ca-Green-1–dextran, and stepped to +40 mV for 1 s, −140 mV for 2 s, and +40 mV again for 1 s from a holding potential of 0 mV. The cell was bathed in normal Ringer except where indicated by the bar showing Ca-free Ringer (0 Ca). IP_3 (23 nl, 1 mM) was injected at the arrow. (a) Time course of development of Cl currents. The outward current during the first +40-mV pulse (+40 mV[1]) is $I_{Cl1\text{-}S}$ (■), the inward current during the −140-mV pulse is I_{Cl2} (○), and the outward current during the second +40-mV pulse (+40 mV[2]) is $I_{Cl1\text{-}T}$ (△) (see Fig. 1 for details). (b) Examples of the current traces at the different time points indicated by a–c in a. (c) Ca fluorescence at each voltage during the experiment. The fluorescence was calculated from the entire confocal section and divided by the initial fluorescence before IP_3 injection. (d) Normalized $I_{Cl1\text{-}S}$ and Ca-dependent fluorescence during the +40 mV[1] step to illustrate the temporal relationship. The inset shows the average time required for both $I_{Cl1\text{-}S}$ and Ca fluorescence at +40 mV[1] to reach one half of their peak value ($t_{1/2}$) ($n = 7$). $I_{Cl1\text{-}S}$ ($t_{1/2} = 0.52 \pm 0.05$) and Ca fluorescence at +40 mV[1] ($t_{1/2} = 3.78 \pm 0.68$) had significantly different rates of decay ($P < 0.0005$). (e) Voltage-dependent Ca fluorescence as a function of time. Voltage-dependent Ca fluorescence was calculated as the difference between F_{Ca}/F_0 at −140 mV and at +40 mV[1]. (f) Correlation between I_{Cl2}, $I_{Cl1\text{-}T}$, and voltage-dependent Ca fluorescence. This cell is representative of seven similar experiments with essentially identical results.

lar (half-times 3.12 ± 0.25 and 3.99 ± 0.56 min, respectively), but I_{Cl2} development was significantly ($P < 0.0055$) slower ($t_{1/2} = 7.2 \pm 0.7$ min) (Fig. 5, e and f). These data agree with our other results showing that $I_{Cl1\text{-}T}$ development parallels the development of I_{SOC}, but that I_{Cl2} develops more slowly (Kuruma and Hartzell, 1999). As was the case when the cell was bathed in Ca-free solution (Fig. 4 d), the fluorescence Ca signal decayed significantly slower ($P < 0.00004$) than $I_{Cl1\text{-}S}$ (Fig. 5 f).

From the data in Figs. 4 and 5, we conclude that in general the correlation between Cl currents and Ca fluorescence is rather poor. Although there are several possible explanations for these data (see DISCUSSION),

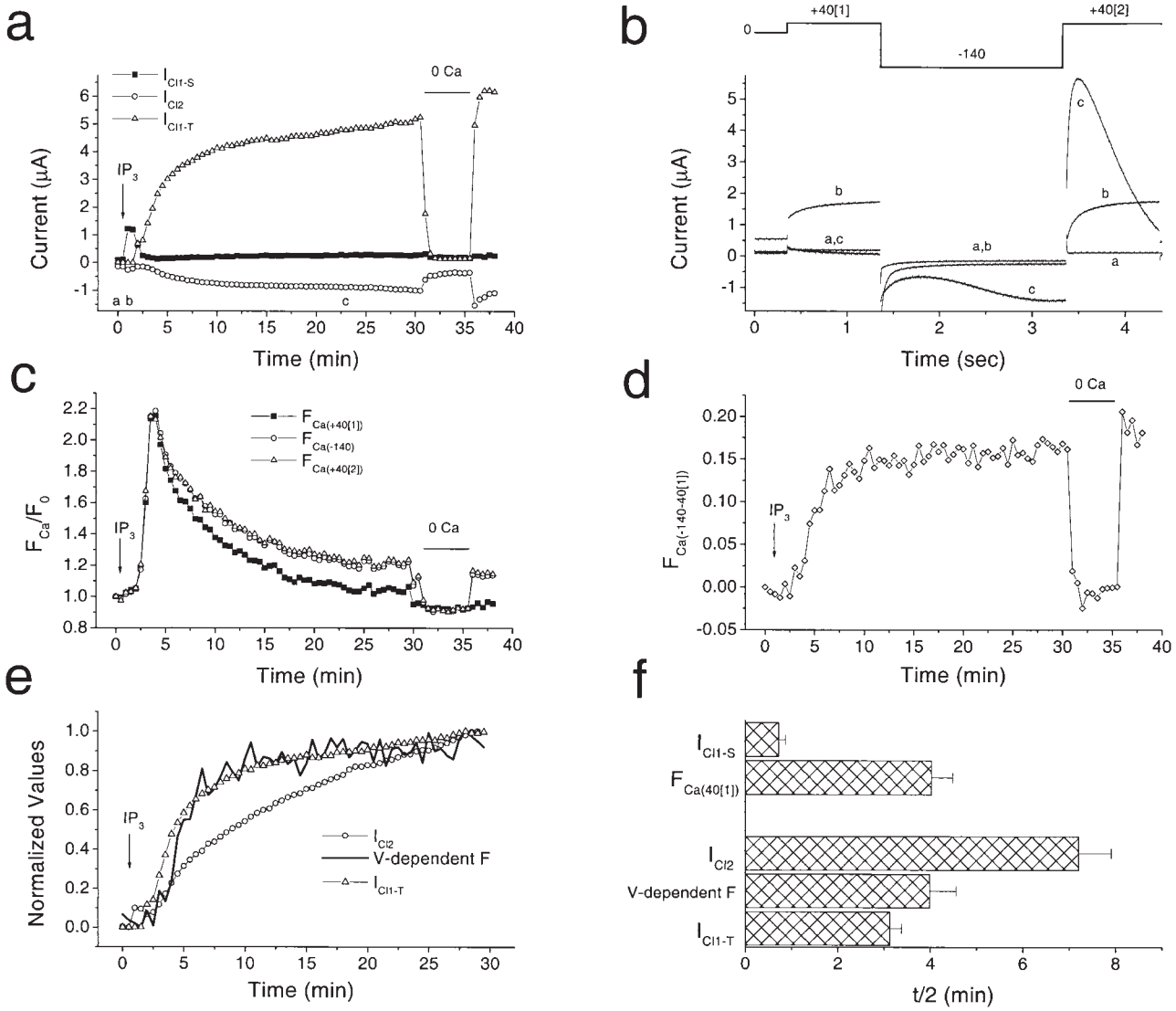

FIGURE 5. Ca transients and Cl currents in normal Ringer. The experimental set up was the same as in Fig. 4 except that the cell was bathed in normal Ringer except where indicated by the bar showing Ca-free Ringer. The point of IP_3 injection (23 nl, 1 mM) is indicated by the arrow. (a) Time course of development of the currents at each voltage. (b) Examples of the current traces at different time points indicated by a–c in a. (c) Ca-dependent fluorescence at each voltage during the experiment. (d) Voltage-dependent Ca fluorescence. (e) Correlation between I_{Cl2}, $I_{Cl1\text{-}T}$, and voltage-dependent Ca fluorescence before switching to Ca-free Ringer. (f) Time required for the currents and Ca fluorescence levels to reach half maximum. For $I_{Cl1\text{-}S}$ and $F_{Ca(+40[1])}$, the time was calculated from the peak and for I_{Cl2}, $I_{Cl1\text{-}T}$, and Ca entry from the point of IP_3 injection. Decay time for $I_{Cl1\text{-}S}$ ($t_{1/2} = 0.72 \pm 0.13$) and $F_{Ca(+40[1])}$ ($t_{1/2} = 4.03 \pm 0.45$) were significantly different ($P < 0.00004$). The time required for $I_{Cl1\text{-}T}$ ($t_{1/2} = 3.12 \pm 0.25$) and Ca entry ($t_{1/2} = 3.99 \pm 0.56$) to reach half maximum value were not significantly different, whereas I_{Cl2} required a significantly ($P < 0.0055$) longer time to reach half maximal value ($t_{1/2} = 7.2 \pm 0.7$) ($n = 6$).

we believe that the data are most simply explained if the Ca fluorescence and the Cl channels report different Ca.

Fast Dynamics of Ca

We then compared Ca fluorescence and Cl currents on a faster time scale. We acquired 15 × 512 pixel images every 100 ms during the voltage-clamp episodes ~10 min after IP_3 injection when SOCE had developed. Fig. 6 a shows the time course of the Ca fluorescence during a standard three-step voltage clamp episode every 30 s from a holding potential of 0 mV. The Ca fluorescence remained stable until the membrane was hyperpolarized to −140 mV, at which time the Ca fluorescence increased as Ca entered the cell. Upon returning to +40 mV[2], the Ca fluorescence began to decline. The decline continued at the same rate when the cell was returned to the 0-mV holding potential. Ca fluores-

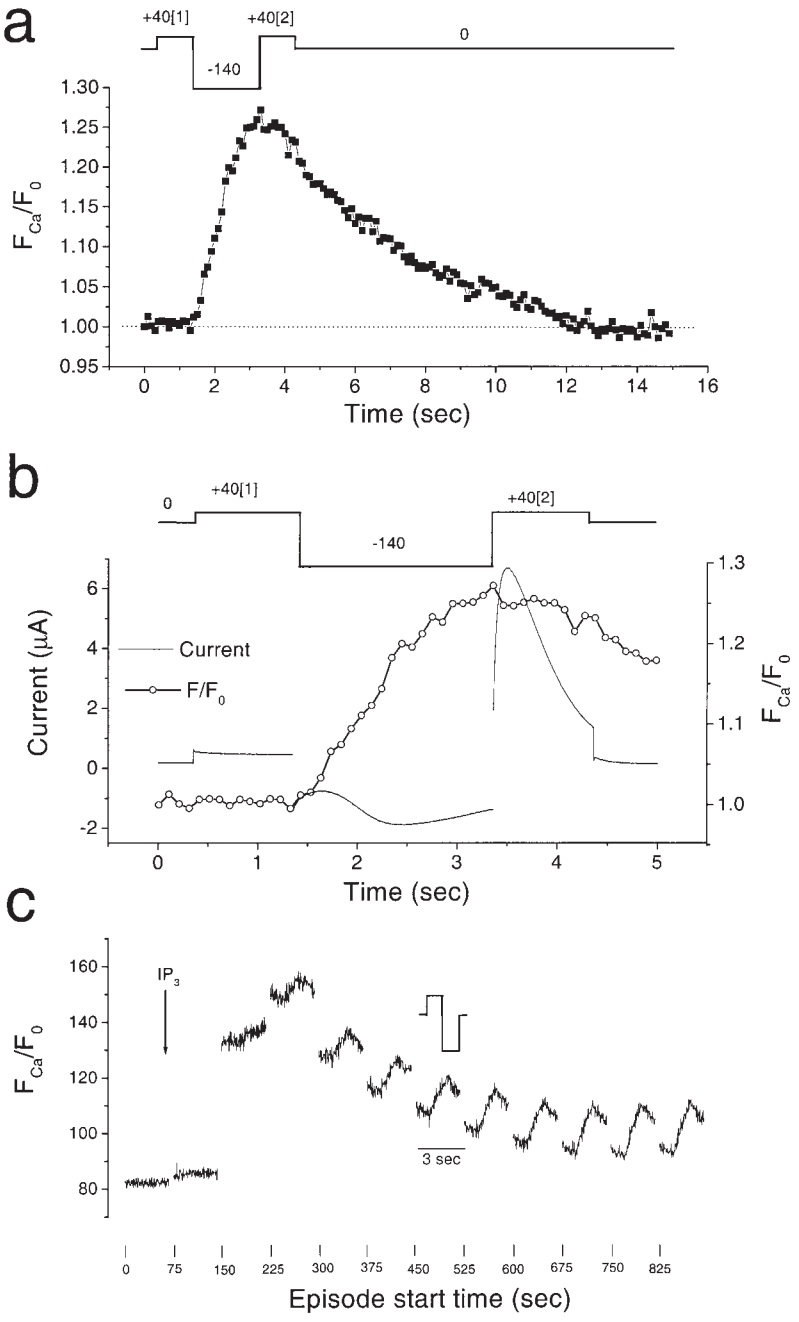

FIGURE 6. Fast Ca dynamics imaged with Ca-green–dextran. The experimental setup was identical to Fig. 5 except that images were collected every 100 ms, starting 400 ms before the +40 mV[1] step from a 15 pixel–wide box across the entire oocyte. The oocyte was injected with $IP_3 >$ 10 min before the experiment. (a) Ca dynamics measured at a fast time scale (every 100 ms). (b) Correlation of Ca fluorescence (○) with the Cl currents (solid line) measured during the same voltage-clamp episode. The Ca fluorescence is superimposed on the Cl currents. (c) Changes in Ca fluorescence traces during the course of an experiment. In this case, we used a two-step voltage protocol, from 0 to +40 mV for 1.5 s, and then to −140 mV for 1.5 s with an interepisode interval of 15 s. Each trace is the average of five consecutive traces. The x axis shows the start time of the beginning of each average trace, but each trace is 3 s in duration and not to scale of the major x axis. After IP_3 injection, Ca-dependent fluorescence increased gradually to reach a maximum ~2 min later. However, the first two traces after IP_3 injection are flat, indicating that there is no significant voltage-dependent Ca entry as Ca is released from the stores. As time progresses, the levels of Ca Green fluorescence at −140 mV, as compared with +40 mV, increase gradually, indicating the development of robust Ca influx.

cence returned to baseline ~10 s after the end of the −140-mV pulse. In Fig. 6 b, Ca fluorescence is superimposed with the current traces on a faster time scale to illustrate the correspondence between Ca fluorescence and Cl currents. Ca fluorescence did not correlate well with the Cl current waveforms. For example, although Ca increased steadily during the −140-mV pulse, I_{Cl2} inactivated partly during the same time period. Furthermore, during the +40 mV[2] pulse, Ca fluorescence declined quite slowly, but $I_{Cl1\text{-}T}$ had completely inactivated.

Fig. 6 c shows 3-s–duration Ca traces (as in Fig. 6 b) taken at 75-s intervals during the time course of an entire experiment before and after IP_3 injection. Before IP_3 injection, the Ca trace was flat at all voltages (first trace). Upon injection of IP_3, the fluorescence increased slightly at all voltages (second trace) and, within 2.5 min (third trace), the Ca fluorescence had increased significantly at all voltages with the fluorescence being slightly greater during the −140 mV and +40 mV[2] pulses. As the Ca fluorescence during the +40 mV[1] step returned toward baseline, the difference in Ca fluorescence between the −140 mV and +40 mV[1] steps became progressively greater as store-operated Ca entry developed. These data confirm our

previous conclusions that SOCE began to develop very early after release of Ca from stores, but that its full development required several minutes.

Ca Fluorescence and Cl Currents Report Spatially Different Ca Concentrations

Figs. 4–6 show that Cl currents and Ca fluorescence do not correlate well. Because Cl channels are at the plasma membrane, they necessarily respond to Ca at the plasmalemma. In contrast, Ca fluorescence is collected from an optical section that includes cytoplasm that may be physiologically remote from the plasmalemma. If the Cl channels and the Ca-sensitive dye are reporting Ca signals that are spatially different, this suggests the presence of Ca gradients between the plasma membrane and cytosol. We performed the following experiments to test the hypothesis that after release of Ca from stores, Ca levels in a layer immediately below the plasma membrane become lower than in the adjacent cytosol because of rapid Ca efflux.

Slowing the inactivation of $I_{Cl1\text{-}S}$ by La. We predicted that if Ca levels immediately below the plasma membrane are lower than in the cytosol because of Ca efflux, inhibition of the plasma membrane efflux pathways would keep subplasmalemmal Ca levels elevated and the decay of $I_{Cl1\text{-}S}$ after release of Ca from stores should be slowed. We tested this prediction by studying the decay of $I_{Cl1\text{-}S}$ in oocytes bathed in control or La^{3+}-containing solutions (1 mM) to inhibit both the plasma membrane Ca-ATPase (Sarkadi et al., 1977) and the Na–Ca exchanger (Kimura et al., 1986) (Fig. 7). La^{3+} at 1 mM has been shown to inhibit ~70% of total Ca efflux (Brommundt and Kavaler, 1987). In control cells, $I_{Cl1\text{-}S}$ inactivated in <2 min, whereas, when Ca efflux was inhibited by La^{3+}, $I_{Cl1\text{-}S}$ required >10 min to return to baseline levels (Fig. 7 a). The $t_{1/2}$ of decay of $I_{Cl1\text{-}S}$ in control (0.55 ± 0.08 min) and La^{3+}-treated (3.62 ± 0.49 min) cells were significantly different ($P < 0.000036$) (Fig. 7 b). Not only did $I_{Cl1\text{-}S}$ last longer in La^{3+}-containing solutions, but its amplitude was ~1.5× greater than that of $I_{Cl1\text{-}S}$ under control conditions. These data are consistent with the hypothesis that inhibition of plasma membrane Ca efflux significantly increased the amplitude and duration of the Ca transient below the plasma membrane.

Ca imaging with lipophilic Ca-sensitive dyes. A direct test of the hypothesis that there are Ca gradients between the bulk cytosol and subplasmalemma would be to image subplasmalemmal Ca. This was done by injecting the lipophilic Ca-sensitive dye Ca-green-C_{18}, which incorporates into membranes with high affinity and has been used to measure Ca in the immediate vicinity of the plasma membrane. We imaged Ca in the plane of the plasma membrane using the smallest scanning pinhole, permitting a z-axis resolution of ~4 μm. Under

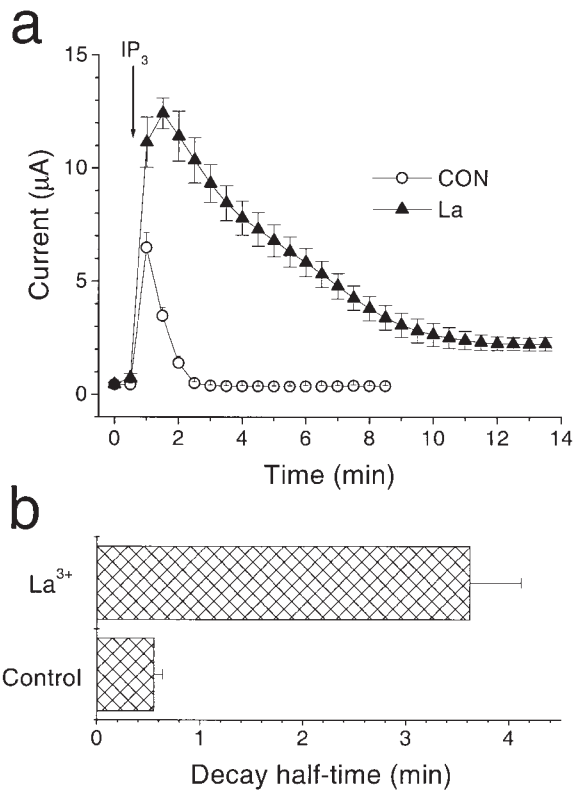

FIGURE 7. Effect of inhibition of Ca efflux with La. Normal oocytes were voltage clamped and injected with IP_3 (23 nl of 1 mM) at the arrow. The voltage protocol was identical to that in Fig. 4. (a) The cells were bathed either in normal Ringer (○) or normal Ringer plus 1 mM La^{3+} (▲). The development of $I_{Cl1\text{-}S}$ (during the +40-mV[1] pulse) is plotted vs. time. (b) Time required for $I_{Cl1\text{-}S}$ to reach half maximum of the peak current level. The time required to reach half maximum value in normal Ringer (control) ($t_{1/2}$ = 0.55 ± 0.08) and in the presence of La^{3+} ($t_{1/2}$ = 3.62 ± 0.49) were significantly different ($P < 0.000036$).

these conditions, we found that the Ca fluorescence increased and decreased much more rapidly than with Ca-green-dextran (Fig. 8 a). The half-time of decay of the Ca fluorescence after the −140 mV pulse was 3.6 ± 0.4 s with Ca-green-dextran and 1.25 ± 0.1 s with Ca-green-C_{18} (Fig. 8 b). Furthermore, the waveform of the Ca fluorescence measured with Ca-green-C_{18} much more closely approximated the waveform of the Cl currents (Fig. 8 c) than the fluorescence measured with Ca-green-dextran (Fig. 6 b). These results support the hypothesis that Ca in the bulk cytosol is different than Ca immediately under the membrane.

If subplasmalemmal Ca is cleared more quickly than the Ca in the bulk cytosol, this would explain why $I_{Cl1\text{-}S}$ turns off within several minutes after an IP_3 injection, whereas Ca fluorescence remains elevated for ~10 min. To test this hypothesis, we imaged Ca-green-C_{18} at the membrane in response to IP_3 injection and found that the membrane Ca signal coincided very closely

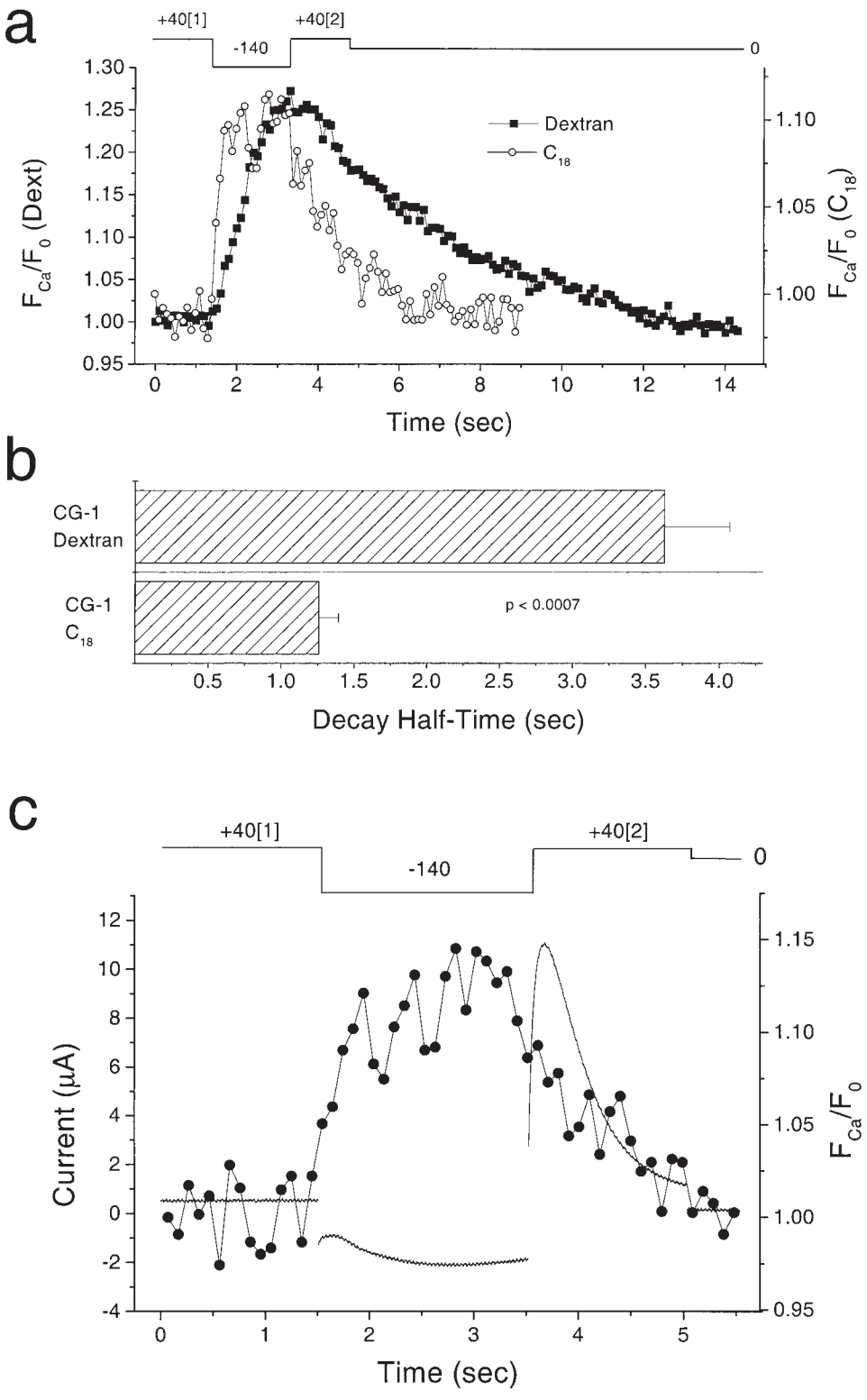

FIGURE 8. Fast Ca dynamics imaged with Ca-green–C_{18}. The experimental setup was identical to Fig. 6 except that the cell was injected with Ca-green–C_{18} instead of Ca-green–dextran, and we imaged from a confocal section 4-μm thick. (a) Ca dynamics measured every 100 ms in an oocyte injected with Ca-green–C_{18} (○) or Ca-green-dextran (■ from Fig. 6). (b) Decay half-time for the Ca signal in a. The time required for the fluorescent signal to decay to one-half of the peak amplitude was measured ($n = 3$). (c) Correlation of the fast Ca dynamics measured by Ca-green–C_{18} fluorescence with Cl currents. The Ca fluorescence (●) and the Cl currents (solid line) from the same voltage clamp episode are superimposed.

with $I_{Cl1\text{-}S}$ (Fig. 9 a). Consequently the half-time of decay of the Ca fluorescence measured with Ca-green-C_{18} was similar to the decay of $I_{Cl1\text{-}S}$ and significantly different ($P < 0.003$) from the decay of the Ca fluorescence measured by Ca-green-dextran (Fig. 9 b). Comparison of the data obtained with Ca-green-dextran and Ca-green-C_{18} show clearly that there is a gradient of Ca between the plasma membrane and the deep cytosol. The Cl channels, as expected, reflect the Ca at the membrane.

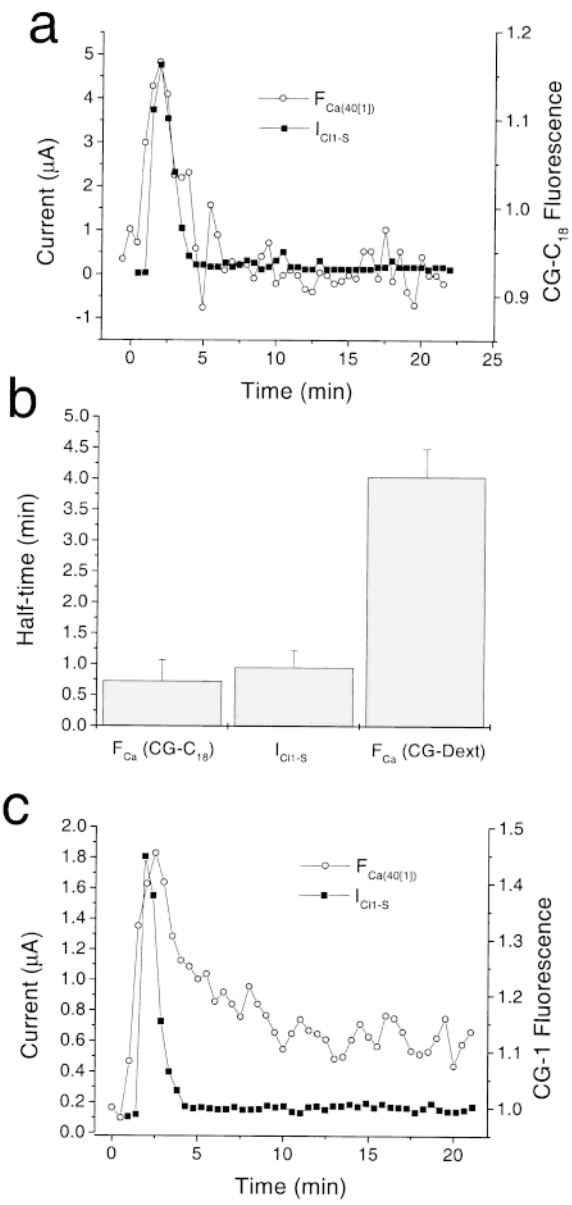

FIGURE 9. Correlation of Ca-green–C_{18} fluorescence with decay of $I_{Cl1\text{-}S}$. The oocyte was injected with Ca-green–C_{18} 30 min before the start of the experiment. (a) IP_3 was injected at $t = 0$ and Ca fluorescence (○) and $I_{Cl1\text{-}S}$ (■) were measured. Because the Cl currents are measured from the entire oocyte, whereas the fluorescence is measured from a very small patch of membrane, the fluorescence trace was shifted ~2 min on the x axis so that its peak coincided with the peak of $I_{Cl1\text{-}S}$ to emphasize the similarity in time course. (b) The time for the current and Ca fluorescence to decay to one half of their peak amplitudes were averaged for four experiments as in a. The half time of Ca fluorescence decay for cells injected with Ca-green–dextran is also shown (from Fig. 5 f). (c) The oocyte was injected with Ca-green-1 coupled to 70 kD dextran and imaged with the same pinhole and confocal settings as the cell in a. As in a, the Ca fluorescence trace was shifted by 1 min on the x axis to make the peaks of $I_{Cl1\text{-}S}$ and Ca fluorescence correspond. IP_3 was injected at $t = 0$. Ca fluorescence (○) decay with a significantly slower time course than $I_{Cl1\text{-}S}$ (■) under these conditions, indicating that the correlation between $I_{Cl1\text{-}S}$ and Ca-green–C_{18} Ca fluorescence is not due to the conditions used to image submembrane Ca.

It should be noted that the amplitudes of the fluorescent signals measured with Ca-green-C_{18} were significantly smaller than those measured with Ca-green-dextran because of the smaller pinhole and the fact that the image was taken from a very superficial optical plane tangential to the plasma membrane. For this reason, the fluorescence traces with Ca-green-C_{18} were noisier than those with Ca-green-dextran. When similar confocal imaging settings (smallest pinhole) were used with cells loaded with Ca-green-dextran, the kinetics of Ca fluorescence were significantly slower than those of $I_{Cl1\text{-}S}$ (Fig. 9 c). Therefore, the fast kinetics observed with Ca-green-C_{18} are not due to the different imaging configuration. This suggests that either the large Ca-green-dextran does not enter the subplasmalemmal space or that it is necessary to have a probe that is closely associated with the plasma membrane to detect the Ca in this localized space.

Recycling of Ca through the ER

The finding that Ca under the plasma membrane is different than in the bulk cytosol raises questions about the mechanisms responsible for establishing this gradient. It is well known that Ca diffusion in the cytosol is much slower than diffusion in simple aqueous solution (Allbritton et al., 1992). If IP_3 injection into the cytoplasm stimulates "instantaneous" release of a bolus of Ca from stores, a wave of Ca will diffuse from the site of injection radially. If efflux of Ca from the cell is faster than the diffusional flux of Ca to the plasmalemma, this would create a Ca gradient with the Ca concentration higher deeper in the cytosol. Diffusional flux of Ca from the cytosol to the subplasmalemmal space could be slowed significantly simply by immobile Ca buffers in the cytosol. However, the possibility existed that uptake of Ca into the endoplasmic reticulum by sarcoplasmic-ER Ca ATPases (SERCAs) also contributed to the slow Ca clearance. To test this hypothesis, we measured the effect of thapsigargin on the rate of decline of Ca fluorescence after IP_3-induced Ca release from stores. We predicted that if SERCAs contribute to the retention of Ca in the cytosol, thapsigargin should accelerate the decay of Ca fluorescence. Fig. 10 shows that the half-time of decline of the Ca fluorescence in control oocytes ($t_{1/2} = 3.78 \pm 0.68$ min, $n = 7$) was 2.4× longer ($P < 0.009$) than in thapsigargin-treated oocytes ($t_{1/2} = 1.48 \pm 0.24$ min, $n = 7$). This result showed that SERCAs play an important role in maintaining elevated Ca levels in the cytosol for prolonged periods of time.

This may seem counterintuitive. Normally, one would expect that SERCA-mediated uptake of Ca into stores would accelerate clearance of Ca from the cytosol, but here SERCA-mediated uptake slows clearance. The reason is that, because of the large IP_3 injection, a large fraction of the IP_3 receptors are open. Neverthe-

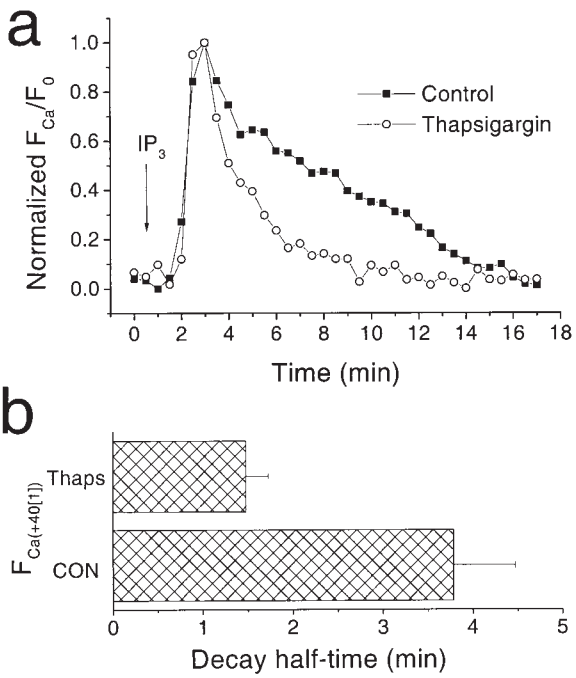

FIGURE 10. Effect of thapsigargin on decay of Ca fluorescence after IP_3 injection. The experimental setup was identical to Fig. 5. IP_3 was injected at the arrow and Ca fluorescence at +40 mV[1] was measured after IP_3 injection (a), and the time required for it to decay to one half of its peak value ($t_{1/2}$) was calculated (b) as in Fig. 4 d. Cells were either treated with DMSO (control) or thapsigargin (Thaps) for 1 h to inhibit the SERCAs without completely depleting the stores. The half time of decay of $F_{Ca(+40[1])}$ was significantly different ($P < 0.009$) between control cells ($t_{1/2}$ = 3.78 ± 0.68, n = 7) and thapsigargin-treated cells ($t_{1/2}$ = 1.48 ± 0.24, n = 7).

less, Ca will be pumped into the ER by the SERCAs, only to be released into the cytosol through the open IP_3 receptors (see DISCUSSION). The uptake of Ca into the ER under these conditions is futile in refilling stores, but clearance of Ca from the cytosol will be greatly slowed because a single Ca molecule may be taken up multiple times in its path towards the plasma membrane, and transient binding to Ca binding proteins in the ER lumen may prolong its residence there.

To test further the idea that the Ca gradients are due to Ca recycling by the ER, we performed the experiments shown in Fig. 11. The rationale of these experiments was to compare Ca fluorescence and Ca-activated Cl currents in control oocytes, oocytes injected with heparin to block Ca release by the IP_3 receptor, and oocytes treated with thapsigargin to block Ca uptake into the ER. Ca stores were depleted by placing the oocytes in Ca-free solution and injecting IP_3 1–2 h before voltage clamping. The oocytes were voltage clamped and the extracellular solution was changed to one containing Ca at the time indicated. Switching control oocytes to Ca-containing solution quickly activated $I_{Cl1\text{-}T}$ and I_{Cl2} (Fig. 11 a) and produced a biphasic increase in Ca fluorescence at all potentials (Fig. 11 b). The initial abrupt increase was voltage dependent, being larger at −140 mV, and thus related to Ca entry. The abrupt increase was followed by a slower increase that was voltage independent, having approximately the same slope at −140 and +40 mV and which continued to increase for >20 min. The voltage-dependent Ca fluorescence increased abruptly upon Ca addition, and then declined slightly over the next 20 min (Fig. 11 c). The decline in Ca entry and in the Cl currents was probably due to partial refilling of ER Ca stores by influxed Ca.

When the oocytes were treated with thapsigargin for >3.5 h to block SERCA-dependent Ca uptake into the ER, a very different profile was observed (Fig. 11, d–f). Addition of Ca to the bath produced an immediate and stable increase in Ca fluorescence during the −140 mV and +40 mV[2] steps. Ca fluorescence during the +40 mV[1] step increased abruptly by a small amount, but then remained steady for ~20 min, as did voltage-dependent Ca entry and $I_{Cl1\text{-}T}$ and I_{Cl2}. This is in marked contrast to the control oocytes, where the Ca fluorescence increased steadily over time. Ca fluorescence traces at +40 mV[1] and −140 mV from thapsigargin-treated oocytes (Fig. 11 e) were superimposed on control Ca fluorescence traces in Fig. 11 b to illustrate the differences in Ca fluorescence changes over time. It is clear that the steady increase in Ca fluorescence observed in control oocytes was eliminated by thapsigargin treatment. The time-dependent increase of the voltage-independent Ca fluorescence ($F_{Ca+40[1]}$) was significantly ($P < 0.047$) greater in control oocytes than in oocytes treated with thapsigargin or heparin. These data show that when SERCAs are active, the level of cytosolic Ca becomes greater with time. These data can be explained if one assumes that transient uptake of Ca into the ER via SERCAs facilitates the retention of Ca in the cytosol. Both the Cl currents ($I_{Cl1\text{-}T}$ and I_{Cl2}) and SOCE activated immediately after Ca addition and remained at steady levels for at least 20 min (Fig. 11, d and f) because inhibition of the SERCAs prohibited Ca uptake into stores.

When oocytes were injected with heparin to block the IP_3 receptor after the stores were depleted, the converse picture was observed (Fig. 11, g–i). Addition of Ca resulted in a transient increase in the Ca fluorescence during the −140 mV and +40 mV[2] steps, but Ca returned to control levels in ~10 min. The transient nature of Ca entry was reflected by the time course of $I_{Cl1\text{-}T}$ and I_{Cl2} (Fig. 11 g). We interpret the transient nature of the Ca fluorescence as being caused by refilling of the Ca stores upon readdition of Ca to the bath. Because the IP_3 receptor was blocked and could not release Ca, the ER was capable of accumulating Ca, and SOCE entry was inactivated. The negative slope in the voltage-

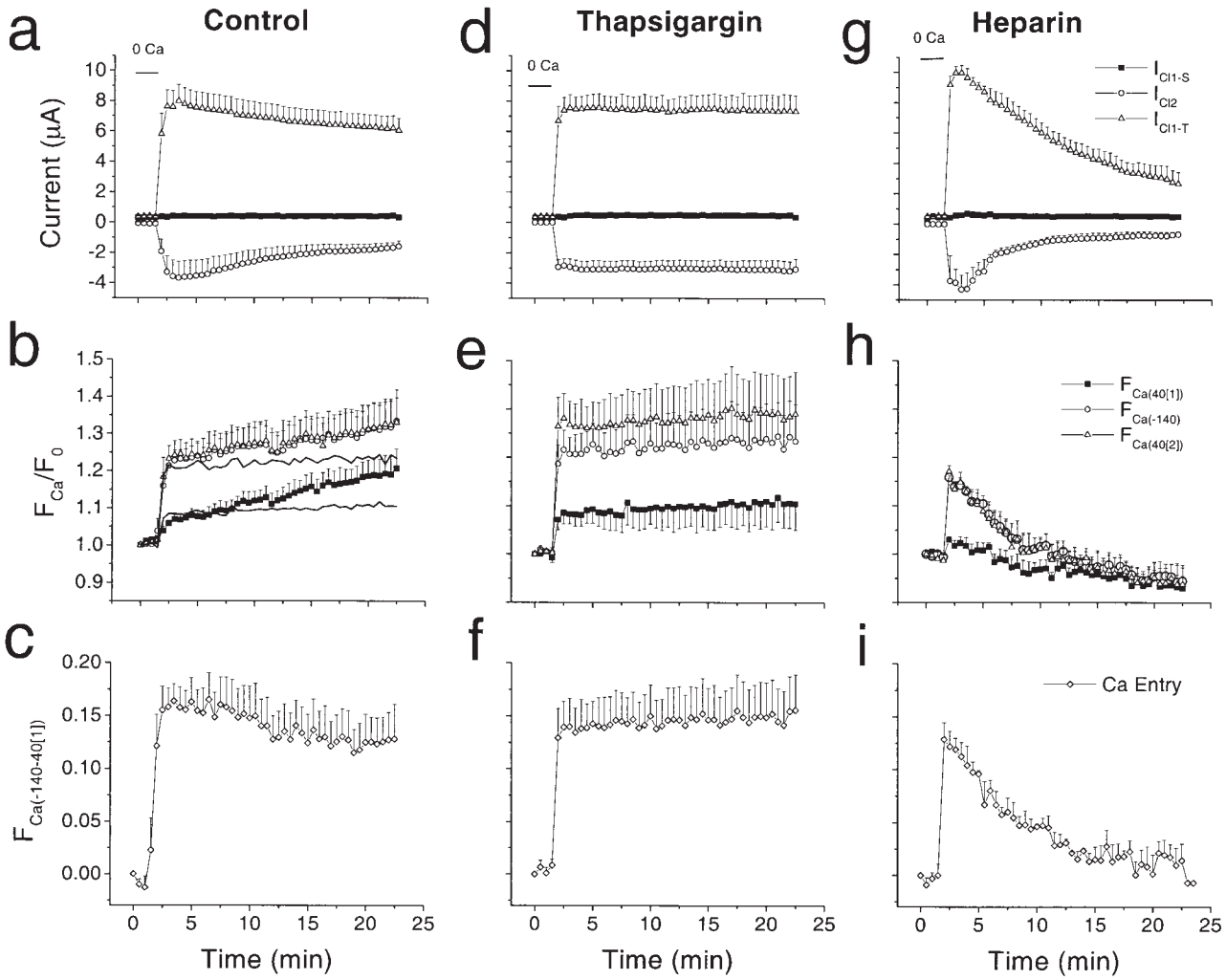

FIGURE 11. Ca recycling through the ER store. Internal Ca stores were depleted by injecting cells with 46 nl of Ca-green–dextran 333 μM + IP_3 50 μM and incubated in nominally Ca-free Ringer for 0.5–2.5 h before the experiment ($n = 6$). Thapsigargin-treated cells (d–f) were preincubated in 1 μM thapsigargin for 3.5 h before IP_3 injection ($n = 7$) and Heparin-treated cells (g–i) were injected with 92 nl 100 μg/μl heparin 15 min before the experiment ($n = 4$). The cells were voltage clamped and stepped to +40 mV for 1.5 s, −140 mV for 2 s, and +40 mV for 1.5 s. a, d, and g represent the time-dependent development of $I_{Cl1\text{-}S}$, I_{Cl2}, and $I_{Cl1\text{-}T}$. b, e, and h show Ca fluorescence at each voltage over time. In b, Ca fluorescence traces at +40 mV[1] and −140 mV from thapsigargin-treated cells (lines, from e) are superimposed on the Ca fluorescence traces under control conditions (symbols) to highlight the difference in slopes. The slopes at +40 mV[1] where significantly ($P < 0.047$) different between control, thapsigargin, and heparin-treated cells. c, f, and i show Ca entry over time.

dependent fluorescence in control and heparin-treated oocytes reflects partial refilling of the stores during the course of the experiment. Refilling is more significant in heparin-treated oocytes because the stores cannot release sequestered Ca.

DISCUSSION

Reversible Ca Gradients Develop between the Plasma Membrane and Cytosol

We conclude that in *Xenopus* oocytes gradients of Ca exist between the cytoplasm and the plasma membrane. When Ca is released from internal stores by injection of IP_3, Ca diffuses from the injection site and activates Ca-activated Cl channels at the plasma membrane. Clearance of Ca from the cytosol is probably mediated under our conditions largely by uptake into mitochondria and efflux into the extracellular space, because accumulation of Ca in the ER is circumvented by the open IP_3 receptors. In our studies, large amounts of IP_3 were injected (initial calculated oocyte concentrations were ~50 μM), and the half-life of IP_3 in *Xenopus* oocytes has been estimated to be between 1 and 10 min, depending on IP_3 and Ca concentration (Shapira et al., 1992; Sims and Allbritton, 1998). In addition, IP_4, which is one of the metabolic products of IP_3, has a lifetime of ~30 min (Sims and Allbritton, 1998) and is also capable of

releasing Ca from stores (Parker and Ivorra, 1990; Ivorra et al., 1991; DeLisle et al., 1995). For these reasons, it seems reasonable to presume that IP_3 receptors remain open for at least tens of minutes under our conditions.

Using Ca-green-dextran and a confocal section including ~35 μm of cytosol below the plasma membrane, we found that the Ca fluorescence after IP_3 injection had a half-time of decay of 1.5 min when Ca uptake into ER stores was blocked with thapsigargin. When SERCAs were not inhibited, the decay was 2.4× slower (Fig. 10 a). This shows that the clearance of Ca from the cytosol was slowed by uptake into the ER. In contrast, the half-time of the Ca signal measured at the plasma membrane with Ca-green-C_{18} was only 0.7 min (Fig. 9 b). This showed clearly that Ca was cleared from the subplasmalemmal space more quickly than from the cytosol further away from the surface. We believe that this gradient arose at least partly because the diffusional supply of Ca released from stores to the plasma membrane was slower than Ca efflux across the plasma membrane. This conclusion was supported by the observation that inhibition of Ca efflux by La, which blocks the plasma membrane Ca-ATPase and Na–Ca exchange, prolongs the rate of decay of the Ca-activated Cl current approximately sevenfold (Fig. 7).

The suggestion that a gradient of Ca exists between the cytosol and the subplasmalemmal space seems reasonable based on known rates of Ca diffusion and the distribution of IP_3 receptors in *Xenopus* oocytes. ER Ca stores, measured by IP_3-receptor immunostaining, are more concentrated close to the plasma membrane in *Xenopus* oocytes (Parys et al., 1992; Kume et al., 1993; Callamara and Parker, 1994). Allbritton et al. (1992) have measured the diffusion coefficient (D) of free Ca in *Xenopus* oocyte cytoplasm as 220 $\mu m^2/s$ when all the Ca buffers are saturated and uptake into organelles is inhibited. Thus, the average time required for a free Ca ion to diffuse to the plasma membrane from a site 50-μm deep in the cytoplasm would be ~2 s ($t = r^2/6D$). If Ca were heavily buffered so that only 1% of the Ca were free at any one time (Neher and Augustine, 1992), the diffusion times would be several minutes ($D_{obs} = D/k$, where k is the ratio of bound/free Ca; Zhou and Neher, 1993). This estimate of a 1–2-min diffusion time corresponds qualitatively with the 1.5-min half-time of Ca clearance we have measured in the presence of thapsigargin. Given this slow diffusion of Ca from the release sites to the plasma membrane, a relatively low density of Ca efflux pathways in the plasma membrane (plasma membrane Ca-ATPase and Na–Ca exchanger) would theoretically be capable of generating a subplasmalemmal Ca gradient. 1 μm^2 of membrane containing 25 Ca transporters, each transporting 250 Ca ions/s could clear ~10^{-20} mol/s. This square micrometer of membrane could reduce the Ca concentration to a depth of 1 μm (1 $\mu m^3 = 10^{-15}$ L) at a rate of 10 μM/s. If Ca release from stores raised cytosolic Ca to 100 μM, this density of transporters could lower the Ca concentration within 1 μm of the membrane to basal levels in ~10 s, if there were no diffusion of Ca into this space from more distant sites. Because the peak concentration of an ion diffusing in an infinite volume decreases proportionally with the cube of the distance (Berg, 1993), Ca released more than several micrometers away from the plasma membrane will not contribute significantly to the Ca concentration in the immediate subplasmalemmal space.

We have clearly demonstrated the existence of a gradient of Ca that develops after release of Ca from stores in which the Ca concentration is lower at the plasma membrane. Our data also support the idea that this gradient changes direction when Ca influx occurs. Our reasons for concluding this are as follows. We have previously shown that I_{Cl2} is less sensitive to Ca than $I_{Cl1\text{-}S}$ (Kuruma and Hartzell, 1999), but the Ca fluorescence reported by cytosolic Ca-green-dextran is less when I_{Cl2} is activated than when $I_{Cl1\text{-}S}$ is activated (Figs. 4 c and 5 c). Furthermore, $I_{Cl1\text{-}T}$ is consistently larger than $I_{Cl1\text{-}S}$. If these currents are mediated by the same type of channel, this would also suggest that Ca concentration is higher at the plasma membrane during Ca entry than occurs in response to Ca release from stores.

An important consideration in our studies of the temporal patterns of Ca distribution was the contribution of the added fluorescent Ca dyes that act as mobile Ca buffers. Neher and Augustine (1992), Zhou and Neher (1993), and Xu et al. (1997) have shown that even small amounts of added mobile Ca buffers dramatically alter the spatio-temporal features of Ca dynamics. We hoped to minimize the contribution of the Ca indicator to the measured Ca dynamics by using relatively immobile Ca indicators, 70-kD–coupled Ca-green-1 and Ca-green-C_{18}, at low concentration. The fact that the kinetics of the Ca-activated Cl currents were very similar between uninjected oocytes and oocytes loaded with the dyes argues that the dyes did not dramatically perturb the normal patterns of Ca distribution or buffering.

Alternative Explanations

The discrepancy between the Ca-green-dextran fluorescence signal and the Cl current could be explained in several ways. Although we prefer the interpretation that the dextran-coupled dye and $I_{Cl1\text{-}S}$ report different Ca signals, there are other possibilities. For example, Parker and co-workers (Parker and Ivorra, 1992, 1993; Parker and Yao, 1994) have suggested that the more rapid turn-off of $I_{Cl1\text{-}S}$ relative to the Ca fluorescence is due to inactivation of the Cl channel. However, we have

shown that the turn off of this current is not caused by an intrinsic inactivation of the channel (Kuruma and Hartzell, 1999). Similarly, one could explain the observation that I_{Cl2} does not turn on in response to Ca release from stores and also turns on more slowly than $I_{Cl1\text{-}T}$ by supposing that this current requires a slow step, such as phosphorylation, for activation. We have shown, however, that this current can be activated very quickly by Ca influx through exogenously expressed iGluR3 channels and have explained its slow activation entirely by its lower sensitivity to Ca than $I_{Cl1\text{-}S}$ and $I_{Cl1\text{-}T}$ (Kuruma and Hartzell, 1999).

We should mention that the data in Fig. 6 a differ somewhat from those reported by Yao and Parker (1993). Yao and Parker (1993) reported that the Ca transient continued to rise after repolarization to 0 mV after a hyperpolarizing step, whereas we found that the Ca signal began to decline immediately upon repolarization. They attribute the increase to Ca-induced Ca release. The difference between their experiments and ours is most likely explained by the fact that we injected $\sim$100$\times$ more IP_3. We found that large IP_3 injections produced a sweeping wave of Ca release that quickly depleted Ca stores, whereas injections similar to those of Yao and Parker (1993) produced regenerative spiral and circular waves of Ca release. With these small injections, Ca stores appeared to refill with Ca shortly after the wave passed, because within seconds Ca could be released from the same locale as another wave passed. Thus, Ca influx under conditions of spiral/circular wave generation would be expected to stimulate release by Ca-induced Ca release. In contrast, when the stores were completely depleted under our conditions, Ca-induced Ca release would be minimal.

Relationship to Other Studies and Significance

Recently, it has become recognized that Ca signals can produce different responses depending on both their amplitude and their frequency (Thomas et al., 1996; Berridge, 1997a). Ca signals in many cells occur as oscillations whose frequency is modulated by agonist concentration. The frequency of the oscillations is related to the magnitude of the cellular response such as secretion or stimulation of enzyme activity (Berridge and Rapp, 1979; Osipchuk et al., 1990; Thorn et al., 1993). Moreover, different regions of the cell, particularly neuronal soma and processes, may exhibit different frequencies of Ca oscillations that elicit qualitatively different responses (Gu and Spitzer, 1995). Certain effectors, such as mitochondrial dehydrogenases, respond best to certain Ca oscillation frequencies because mitochondria behave as high-pass filters for the Ca signals (Hajnoczky et al., 1995; Rutter et al., 1996), but other effectors respond to different Ca oscillation frequencies by mechanisms that remain poorly understood (Dolmetsch et al., 1998). Furthermore, different effectors discriminate between different Ca signals by virtue of differences in their spatial location and their sensitivity to Ca. Probably the best understood examples come from studies of how Ca dynamics can differentially activate transcription. In AtT20 and hippocampal cells, spatially distinct Ca signals in the cytoplasm and nucleoplasm can differentially activate transcription from the serum or cAMP response elements (Bito et al., 1997; Hardingham et al., 1997). In B lymphocytes, high amplitude transient Ca signals are sufficient to produce translocation of the nuclear factor (NF) kB transcription factor into the nucleus, whereas low amplitude sustained Ca signals are required for persistent translocation of NFAT (Dolmetsch et al., 1997).

Our present studies provide a novel example of how Ca signals with different spatial and amplitude characteristics can differentially alter effector (I_{Cl1} and I_{Cl2}) activity. Cytoplasmic Ca gradients have been shown to be physiologically important in a variety of other systems, including unidirectional fluid secretion in pancreatic acinar cells (Kasai and Augustine, 1990), the activation of the transcription factor NFAT (Dolmetsch et al., 1997), regulation of cytoskeleton in migrating cells (Brundage et al., 1991), regulation of ion channel activity (Hoth et al., 1997; De Koninck and Schulman, 1998), and vesicular neurotransmitter release (Neher, 1998). In the case of the *Xenopus* oocyte, these gradients exhibit several particularly interesting features. First, the gradient arises partly because of slowed Ca clearance due to recycling of Ca through the ER stores. Second, the gradients are rapidly reversible depending on the membrane potential. Third, because inward and outward Cl currents have different sensitivity to Ca, these changing gradients produce complex Cl current waveforms. Although the oocyte is an atypically large cell, the gradients that we have described are occurring on the micrometer scale and are likely to also exist in smaller mammalian cells.

The Ca-activated Cl currents in *Xenopus* oocytes are important physiologically: they are responsible for the depolarizing fertilization potential that provides a fast block to polyspermy in *Xenopus* eggs (Jaffe and Cross, 1986). Sperm–egg fusion stimulates IP_3 production and Ca release from stores (Snow et al., 1996), followed by activation of Cl currents that closely resemble $I_{Cl1\text{-}S}$ and I_{Cl2} (D. Glahn and R. Nuccitelli, personal communication). The resting potential of *Xenopus* eggs is usually near -60 mV. Since amphibian eggs in the wild are fertilized in fresh water having relatively low $[Cl^-]$, E_{Cl} is positive, and activation of Cl currents will depolarize the egg. However, Kuruma and Hartzell (1999) have shown that when cytosolic Ca is elevated only moderately, the resulting Cl current is strongly outwardly recti-

fying ($I_{Cl1\text{-}S}$) such that at −60 mV there would be relatively little Cl current. With larger increases in cytosolic Ca, inward current (I_{Cl2}) is also stimulated, which would depolarize the oocyte. This may be an important mechanism to prevent the oocyte from undergoing the fast block to polyspermy prematurely. Small elevations in cytosolic Ca would not have a significant influence on inward Cl currents at the resting potential, but large Ca rises would stimulate Cl current at all potentials, effectively voltage clamping the membrane of the oocyte at E_{Cl} and preventing polyspermy.

We thank Akinori Kuruma for the I_{SOC} current–voltage data in Fig. 2 b, David Glahn and Rich Nuccitelli for access to not yet published material, and David Clapham, Anant Parekh, Reinhold Penner, Lynne Quarmby, Julio Hernandez, Thomas Fisher, and Akinori Kuruma for helpful comments at various stages during these studies.

This work was supported by National Institutes of Health grants GM-55276 and HL-21195.

Original version received 6 October 1998 and accepted version received 2 November 1998.

REFERENCES

Allbritton, N.L., T. Meyer, and L. Stryer. 1992. Range of messenger action of calcium ion and inositol 1,4,5-trisphosphate. *Science.* 258:1812–1815.

Berg, H.C. 1993. Random Walks in Biology. Princeton University Press, Princeton, NJ. 152 pp.

Berridge, M.J. 1988. Inositol triphosphate-induced membrane potential oscillations in *Xenopus* oocytes. *J. Physiol. (Camb.).* 403: 589–599.

Berridge, M.J. 1997a. Elementary and global aspects of calcium signalling. *J. Physiol. (Camb.).* 499:291–306.

Berridge, M.J. 1997b. The AM and FM of calcium signalling. *Nature.* 386:759–760.

Berridge, M.J., and P.E. Rapp. 1979. A comparative survey of the function, mechanism and control of cellular oscillators. *J. Exp. Biol.* 81:217–279.

Bezprozvanny, I., J. Watras, and B.E. Ehrlich. 1991. Bell-shaped calcium-response curves of Ins(1,4,5)P3 and calcium-gated channels from endoplasmic reticulum of cerebellum. *Nature.* 351: 751–754.

Bird, G., H. Takemura, O. Thastrup, J. Putney, and F. Menniti. 1992. Mechanisms of activated Ca^{2+} entry in the rat pancreatoma cell line, AR4-2J. *Cell Calc.* 13:49–58.

Bito, H., K. Deisseroth, and R.W. Tsien. 1997. Ca^{2+}-dependent regulation in neuronal gene expression. *Curr. Opin. Neurobiol.* 7:429.

Boton, R., N. Dascal, B. Gillo, and Y. Lass. 1989. Two calcium-activated chloride conductances in *Xenopus laevis* oocytes permeabilized with the ionophore A23187. *J. Physiol. (Camb.).* 408:511–534.

Brommundt, G., and F. Kavaler. 1987. La^{3+}, Mn^{2+}, and Ni^{2+} effects on Ca^{2+} pump and on Na^{+}–Ca^{+} exchange in bullfrog ventricle. *Am. J. Physiol.* 253:C45–C51.

Brundage, R.A., K.E. Fogarty, R.A. Tuft, and F.S. Fay. 1991. Calcium gradients underlying polarization and chemotaxis of eosinophils. *Science.* 254:703–706.

Callamara, N., and I. Parker. 1994. Inositol 1,4,5-trisphosphate receptors in *Xenopus laevis* oocytes: localization and modulation by Ca^{2+}. *Cell Calc.* 15:66–78.

Camacho, P., and J. Lechleiter. 1993. Increased frequency of calcium waves in *Xenopus laevis* oocytes that express a calcium-ATPase. *Science.* 260:226–229.

Dascal, N. 1987. The use of *Xenopus* oocytes for the study of ion channels. *CRC Crit. Rev. Biochem.* 22:317–387.

De Koninck, P., and H. Schulman. 1998. Sensitivity of CaM kinase II to the frequency of Ca^{2+} oscillations. *Science.* 279:227–230.

Deisseroth, K., E.K. Heist, and R.W. Tsien. 1998. Translocation of calmodulin to the nucleus supports CREB phosphorylation in hippocampal neurons. *Nature.* 392:202.

DeLisle, S., G.W. Mayr, and M.J. Welsh. 1995. Inositol phosphate structural requisites for Ca^{2+} influx. *Am. J. Physiol.* 268:C1485–C1491.

Dolmetsch, R.E., R.S. Lewis, C.C. Goodnow, and J.I. Healy. 1997. Differential activation of transcription factors induced by Ca response amplitude and duration. *Nature.* 386:855–858.

Dolmetsch, R.E., K. Xu, and R.S. Lewis. 1998. Calcium oscillations increase the efficiency and specificity of gene expression. *Nature.* 392:933–936.

Finch, E.A., T.J. Turner, and S.M. Goldin. 1991. Calcium as a coagonist of inositol 1,4,5-trisphosphate-induced calcium release. *Science.* 252:443–446.

Finkbeiner, S., and M.E. Greenberg. 1996. Ca^{2+}-dependent routes to Ras: mechanisms for neuronal survival, differentiation, and plasticity? *Neuron.* 16:233–236.

Ghosh, A., and M.E. Greenberg. 1995. Calcium signaling in neurons: molecular mechanisms and cellular consequences. *Science.* 268:239–247.

Gillo, B., Y. Lass, E. Nadler, and Y. Oron. 1987. The involvement of inositol 1,4,5-triphosphate and calcium in the two-component response to acetylcholine in *Xenopus* oocytes. *J. Physiol. (Camb.).* 392:349–361.

Girard, S., and D. Clapham. 1993. Acceleration of intracellular calcium waves in *Xenopus* oocytes by calcium influx. *Science.* 260: 229–232.

Gu, X., and N. Spitzer. 1995. Distinct aspects of neuronal differentiation encoded by frequency of spontaneous Ca transients. *Nature.* 375:784–787.

Hajnoczky, G., L.D. Robb-Gaspars, M.B. Seitz, and A.P. Thomas. 1995. Decoding of cytosolic calcium oscillations in the mitochondria. *Cell.* 82:415–424.

Hardingham, G., S. Chawla, G. Johnson, and H. Bading. 1997. Distinct functions of nuclear and cytoplasmic calcium in the control of gene expression. *Nature.* 385:260–265.

Hartzell, H.C. 1996. Activation of different Cl currents in *Xenopus* oocytes by Ca liberated from stores and by capacitative Ca influx. *J. Gen. Physiol.* 108:157–175.

Hoth, M., C. Fanger, and R.S. Lewis. 1997. Mitochondrial regulation of store-operated calcium signaling in T lymphocytes. *J. Cell Biol.* 137:633–648.

Hoth, M., and R. Penner. 1993. Calcium release-activated calcium current in rat mast cells. *J. Physiol. (Camb.).* 465:359–386.

Iino, M. 1990. Biphasic Ca^{2+} dependence of inositol 1,4,5-trisphosphate-induced Ca release in smooth muscle cells of the guinea

pig Taenia Caeci. *J. Gen. Physiol.* 95:1103–1122.

Ivorra, I., R. Gigg, R.F. Irvine, and I. Parker. 1991. Inositol 1,3,4,6-tetrakisphosphate mobilizes calcium in *Xenopus* oocytes with high potency. *Biochem. J.* 273:317–321.

Jaffe, L.A., and N.L. Cross. 1986. Electrical regulation of sperm-egg fusion. *Annu. Rev. Physiol.* 48:191–200.

Jouaville, L.S., F. Ichas, E.L. Holmuhamedov, P. Camacho, and J.D. Lechleiter. 1995. Synchronization of calcium waves by mitochondrial substrates in *Xenopus laevis* oocytes. *Nature.* 377:438–441.

Kasai, H., and G. Augustine. 1990. Cytosolic Ca^{2+} gradients triggering unidirectional fluid secretion from exocrine pancreas. *Nature.* 348:735–738.

Kimura, J., A. Noma, and H. Irisawa. 1986. Na-Ca exchange current in mammalian heart cells. *Nature.* 319:596–597.

Kume, S., A. Muto, J. Aruga, T. Nakagawa, T. Michikawa, T. Furuichi, S. Nakade, H. Okano, and K. Mikoshiba. 1993. The *Xenopus* IP_3 receptor: structure, function, and localization in oocytes and eggs. *Cell.* 73:555–570.

Kuruma, A., and H.C. Hartzell. 1999. Dynamics of calcium regulation of Cl currents in *Xenopus* oocytes. *Am. J. Physiol.* 276:C161–C175.

Landolfi, B., S. Curci, L. Debellis, T. Pozzan, and A.M. Hofer. 1998. Ca^{2+} homeostasis in the agonist-sensitive internal store: functional interactions between mitochondria and the ER measured in situ in intact cells. *J. Cell Biol.* 142:1235–1243.

Lechleiter, J.D., and D.E. Clapham. 1992. Molecular mechanisms of intracellular calcium excitability in *X. laevis* oocytes. *Cell.* 69: 283–294.

Lenzi, D., and W.M. Roberts. 1994. Calcium signalling in hair cells: multiple roles in a compact cell. *Curr. Opin. Neurobiol.* 4:496–502.

Luby-Phelps, K. 1989. Preparation of fluorescently labeled dextrans and ficolls. *Methods Cell Biol.* 29:59–73.

Machaca, K., and H.C. Hartzell. 1998. Asymmetrical distribution of Ca-activated Cl channels in *Xenopus* oocytes. *Biophys. J.* 74:1286–1295.

Meldolesi, J., E. Clementi, C. Fasolato, D. Zacchetti, and T. Pozzan. 1991. Ca^{2+} influx following receptor activation. *Trends Pharmacol. Sci.* 12:289–292.

Miledi, R., and I. Parker. 1984. Chloride current induced by injection of calcium into *Xenopus* oocytes. *J. Physiol. (Camb.).* 357:173–183.

Morgan, A.J., and R. Jacob. 1994. Ionomycin enhances Ca^{2+} influx by stimulating store-regulated cation entry and not by a direct action at the plasma membrane. *Biochem. J.* 300:665–672.

Neher, E. 1998. Vesicle pools and Ca^{2+} microdomains: new tools for understanding their roles in neurotransmitter release. *Neuron.* 20:389–399.

Neher, E., and G.J. Augustine. 1992. Calcium gradients and buffers in bovine chromaffin cells. *J. Physiol. (Camb.).* 450:273–301.

Osipchuk, Y.V., M. Wakai, D.I. Yule, D.V. Gallacher, and O.H. Petersen. 1990. Cytoplasmic Ca^{2+} oscillations evoked by receptor stimulation, G-protein activation, internal application of inositol trisphosphate of Ca^{2+}: simultaneous microfluorimetry and Ca^{2+} dependent Cl^- current recording in single pancreatic acinar cells. *EMBO (Eur. Mol. Biol. Organ.) J.* 9:697–704.

Parekh, A.B., and R. Penner. 1997. Store depletion and calcium influx. *Physiol. Rev.* 77:901–930.

Parker, I., C.B. Gundersen, and R. Miledi. 1985. A transient inward current elicited by hyperpolarization during serotonin activation in *Xenopus* oocytes. *Proc. R. Soc. Lond. B Biol. Sci.* 223:279–292.

Parker, I., and I. Ivorra. 1990. Localized all-or-none calcium liberation by inositol trisphosphate. *Science.* 250:977–979.

Parker, I., and I. Ivorra. 1991. Inositol tetrakisphosphate liberates stored Ca^{2+} in *Xenopus* oocytes and facilitates responses to inositol trisphosphates. *J. Physiol. (Camb.).* 433:207–227.

Parker, I., and I. Ivorra. 1992. Characteristics of membrane currents evoked by photoreleased inositol trisphosphate in *Xenopus* oocytes. *Am. J. Physiol.* 263:C154–C165.

Parker, I., and I. Ivorra. 1993. Confocal microfluorimetry of Ca^{2+} signals evoked in *Xenopus* oocytes by photoreleased inositol trisphosphate. *J. Physiol. (Camb.).* 461:133–165.

Parker, I., and R. Miledi. 1987a. Injection of inositol 1,3,4,5-tetrakisphosphate into *Xenopus* oocytes generates a chloride current dependent upon intracellular calcium. *Proc. R. Soc. Lond. B Biol. Sci.* 232:59–70.

Parker, I., and R. Miledi. 1987b. Inositol trisphosphate activates a voltage-dependent calcium influx in *Xenopus* oocytes. *Proc. R. Soc. Lond. B Biol. Sci.* 231:27–36.

Parker, I., and Y. Yao. 1994. Relation between intracellular Ca^{2+} signals and Ca^{2+}-activated Cl^- current in *Xenopus* oocytes. *Cell Calc.* 15:276–288.

Parys, J.B., S.W. Sernett, S. DeLisle, P.M. Snyder, M.J. Welsh, and K.P. Campbell. 1992. Isolation, characterization, and localization of the inositol 1,4,5-trisphosphate receptor protein in *Xenopus laevis* oocytes. *J. Biol. Chem.* 267:18776–18782.

Pozzan, T., R. Rizzuto, P. Volpe, and J. Meldolesi. 1994. Molecular and cellular physiology of intracellular stores. *Physiol. Rev.* 74: 595–636.

Putney, J.W., Jr. 1986. A model for receptor-regulated calcium entry. *Cell Calc.* 7:1–12.

Putney, J.W., Jr. 1990. Capacitative calcium entry revisited. *Cell Calc.* 11:611–624.

Quarmby, L.M., and H.C. Hartzell. 1994. Dissection of eukaryotic transmembrane signalling using *Chlamydomonas. Trends Pharmacol. Sci.* 15:343–349.

Ríos, E., and M.D. Stern. 1997. Calcium in close quarters: microdomain feedback in excitation–contraction coupling and other cell biological phenomena. *Annu. Rev. Biophys. Biomol. Struct.* 26: 47–82.

Rutter, G.A., P. Burnett, R. Rizzuto, M. Brini, M. Murgia, T. Pozzan, J.M. Tavare, and R.M. Denton. 1996. Subcellular imaging of intramitochondrial Ca^{2+} with recombinant targeted aequorin: significance for the regulation of pyruvate dehydrogenase activity. *Proc. Natl. Acad. Sci. USA.* 93:5489–5494.

Sarkadi, B., I. Szasz, A. Gerloczi, and G. Gardos. 1977. Transport parameters and stoichiometry of active calcium extrusion in intact human red cells. *Biochim. Biophys. Acta.* 464:93–107.

Shapira, H., M. Lupu-Meiri, and Y. Oron. 1992. The metabolism of microinjected inositol trisphosphate in *Xenopus* oocytes. *J. Basic Clin. Physiol. Pharmacol.* 3:119–138.

Sims, C.E., and N.L. Allbritton. 1998. Metabolism of inositol 1,4,5-trisphosphate and inositol 1,3,4,5-tetrakisphosphate by the oocytes of *Xenopus laevis. J. Biol. Chem.* 273:4052–4058.

Snow, P., D.L. Yim, J.D. Leibow, S. Saini, and R. Nuccitelli. 1996. Fertilization stimulates an increase in inositol trisphosphate and inositol lipid levels in *Xenopus* eggs. *Dev. Biol.* 180:108–118.

Snyder, P.M., K. Krause, and M.J. Welsh. 1988. Inositol triphosphate isomers, but not inositol 1,3,4,5-tetrakisphosphate, induce calcium influx in *Xenopus laevis* oocytes. *J. Biol. Chem.* 263:11048–11051.

Thomas, A.P., G.St.J. Bird, G. Hajnoczky, L.D. Robb-Gaspars, and J.W. Putney, Jr. 1996. Spatial and temporal aspects of cellular calcium signalling. *FASEB. J.* 10:1517.

Thorn, P. 1996. Spatial domains of Ca^{2+} signaling in secretory epithelial cells. *Cell Calc.* 20:214.

Thorn, P., A.M. Lawrie, P.M. Smith, D.V. Gallacher, and O.H. Petersen. 1993. Ca^{2+} oscillations in pancreatic acinar cells: spatiotemporal relationships and functional implications. *Cell Calc.* 14:746–757.

Xu, T., M. Naraghi, H. Kang, and E. Neher. 1997. Kinetic studies of

Ca^{2+} binding and Ca^{2+} clearance in the cytosol of adrenal chromaffin cells. *Biophys. J.* 73:532–545.

Yao, Y., and I. Parker. 1993. Inositol trisphosphate-mediated Ca^{2+} influx into *Xenopus* oocytes triggers Ca^{2+} liberation from intracellular stores. *J. Physiol. (Camb.).* 468:275–296.

Yao, Y., and I. Parker. 1994. Ca^{2+} influx modulation of temporal and spatial patterns of inositol trisphosphate-mediated Ca^{2+} liberation in *Xenopus* oocytes. *J. Physiol. (Camb.).* 476:17–28.

Yao, Y., and R.Y. Tsien. 1997. Calcium current activated by depletion of calcium stores in *Xenopus* oocytes. *J. Gen. Physiol.* 109:703–715.

Zhou, Z., and E. Neher. 1993. Mobile and immobile calcium buffers in bovine adrenal chromaffin cells. *J. Physiol. (Camb.).* 469: 245–273.